J. Fluid Mech. (1998), *vol.* 356, *pp.* 353–379. Printed in the United Kingdom

Effects of the Coriolis force on the stability of Stuart vortices

By STÉPHANE LEBLANC AND CLAUDE CAMBON

Laboratoire de Mécanique des Fluides et d'Acoustique, UMR 5509 CNRS
Ecole Centrale de Lyon, BP 163, 69131 Ecully Cedex, France

(Received 16 December 1996 and in revised form 9 September 1997)

A detailed investigation of the effects of the Coriolis force on the three-dimensional linear instabilities of Stuart vortices is proposed. This exact inviscid solution describes an array of co-rotating vortices embedded in a shear flow. When the axis of rotation is perpendicular to the plane of the basic flow, the stability analysis consists of an eigenvalue problem for non-parallel versions of the coupled Orr–Sommerfeld and Squire equations, which is solved numerically by a spectral method. The Coriolis force acts on instabilities as a 'tuner', when compared to the non-rotating case. A weak anticyclonic rotation is destabilizing: three-dimensional Floquet modes are promoted, and at large spanwise wavenumber their behaviour is predicted by a 'pressureless' analysis. This latter analysis, which has been extensively discussed for simple flows in a recent paper (Leblanc & Cambon 1997) is shown to be relevant to the present study. The basic mechanism of short-wave breakdown is a competition between instabilities generated by the elliptical cores of the vortices and by the hyperbolic stagnation points in the braids, in accordance with predictions from the 'geometrical optics' stability theory. On the other hand, cyclonic or stronger anticyclonic rotation kills three-dimensional instabilities by a cut-off in the spanwise wavenumber. Under rapid rotation, the Stuart vortices are stabilized, whereas inertial waves propagate.

1. Introduction

The present study deals with linear inviscid instabilities of plane flows in an incompressible homogeneous rotating fluid. The angular velocity vector $\boldsymbol{\Omega} = \Omega \boldsymbol{e}_z$ of the rotating frame is considered perpendicular to the plane of the basic flows. Because of the wide variety of physical phenomena triggered by the Coriolis force (some basic mechanisms are briefly described by Batchelor 1967, pp. 555–567; and extensive analyses may be found in Greenspan 1969), the present study may be introduced by three different questions, which in fact are linked.

The first one deals with the three-dimensional nature of the instabilities, since two-dimensional motions in the plane of the basic flow are unaffected by the Coriolis force. In an inertial frame, three-dimensional instabilities were widely studied in the early 1980s with the 'Orszag/Herbert' transition mechanism in shear flows (see the reviews in Bayly, Orszag & Herbert 1988; Herbert 1988). It may be summarized as follows: *"the initial parallel flow is the wrong state to linearize about if we wish to understand the origin of complex three-dimensional structure; the correct state is a nonlinear equilibrium or quasi-equilibrium arising from the primary instability"* (Bayly *et al.* 1988). In these works, it was found that two-dimensional basic states or finite-amplitude travelling waves may exhibit three-dimensional linear secondary instabilities

with common generic features, namely short-wavelength fast growing modes resulting from an inertial mechanism: the ellipticity of the streamlines in vortical regions of the non-parallel basic flow is taken to be responsible, and the broadband 'elliptical instability' (Pierrehumbert 1986; Bayly 1986; Landman & Saffman 1987; Waleffe 1989, 1990; Leweke & Williamson 1998; Sipp & Jacquin 1997; and others) is often seen to be a generic model of these instabilities. It seems today that Orszag/Herbert's transition could be 'bypassed' by other mechanisms (see reviews by Henningson 1995; Waleffe 1995). However, the first question is: what are the effects of the Coriolis force on the secondary instabilities of non-parallel shear flows, and does the elliptical instability also play a crucial role in a rotating fluid (Craik 1989; Gledzer & Ponomarev 1992; Smyth & Peltier 1994; Cambon *et al.* 1994)? And what about the role of hyperbolic stagnation points brought to light using exactly the same formalism in the context of rapid distortion theory (RDT) of homogeneous turbulence (Batchelor & Proudman 1954; Cambon 1982; Cambon, Teissèdre & Jeandel 1985; Cambon *et al.* 1994; and others), and more recently in the context of hydrodynamic stability theory (Lagnado, Phan-Thien & Leal 1984; Craik & Criminale 1986; Friedlander & Vishik 1991; Lifschitz & Hameiri 1991)? Do they have a link with the braid longitudinal vortices in plane shear flows and bluff-body wakes (Ho & Huerre 1984; Klaassen & Peltier 1985, 1989, 1991; Metcalfe *et al.* 1987; Lasheras & Choi 1988; Williamson 1996)?

The second issue is linked to the presence of quasi-two-dimensional coherent vortices aligned with the rotation axis. Experimental evidence of such structures is extensive (see the review by Hopfinger & van Heijst 1993). In a rotating tank, diffusive turbulence produced by an oscillating grid leads, above a certain distance from the grid, to the formation of 'long-lived' coherent vortices, which do not emerge in the non-rotating case (Hopfinger, Browand & Gagne 1982; Lollini 1997). Other laboratory experiments have shown the existence of two-dimensional vortices with various complex topologies such as monopolar, dipolar, tripolar and triangular vortices, sometimes observed in direct numerical simulations of two-dimensional turbulence (Kloosterziel 1990; Kloosterziel & van Heijst 1991; van Heijst, Kloosterziel & Williams 1991; Carnevale & Kloosterziel 1994). Emergence of columnar vortices is outside the scope of the present paper because it involves complex mechanisms that cannot be explained by the Taylor–Proudman theorem, which only concerns a linear and steady regime. Thus, in rotating homogeneous turbulence, Cambon, Mansour & Godeferd (1997) have shown that the linear regime which consists of inertial waves cannot explain the transition from three-dimensional to two-dimensional turbulence, which is ultimately triggered by nonlinear interactions (for the crucial role of resonant inertial waves, see also Waleffe 1993; Babin, Mahalov & Nicolaenko 1996). However, the long persistence of these structures suggest that they are insensitive (or stable) to perturbations with rapid growth rate. Are linear mechanisms able to explain the *"presence of intense cyclonic vortices and (much) weaker anticyclonic vortices"* as observed by Hopfinger *et al.* (1982) and others in rotating fluids (Kloosterziel 1990; Bidokhti & Tritton 1992; Smyth & Peltier 1994)?

The third and last question, which in fact links the two previous ones, deals with the generic character of instability mechanisms triggered by the Coriolis force. For parallel shear flows (Pedley 1969; Tritton & Davies 1981), circular vortices (or curved shear flows) (Kloosterziel 1990; Kloosterziel & van Heijst 1991; Mutabazi, Normand & Wesfreid 1992), or quadratic flows (Cambon 1982; Cambon *et al.* 1985, 1994; Craik 1989), there exist exact stability criteria, or more precisely sufficient conditions for instability. Leblanc & Cambon (1997, referred hereafter as LC97), have shown that they may be expressed solely by the second invariant of the 'inertial tensor'. This

'general discriminant' appears as a catalyst of short-wavelength instabilities, which are described at first order by the 'pressureless' dynamics, as already pointed out by Bayly (1988) for the classical centrifugal instability. Moreover, for complex vortical flows, using the 'geometrical optics' stability theory developed and applied recently to fluid mechanics by Lifschitz and coworkers (Lifschitz & Hameiri 1991; Lifschitz 1991, 1994; Bayly, Holm & Lifschitz 1996; Lebovitz & Lifschitz 1996), the role of stagnation points in rotating flows has been clarified (Leblanc 1997). Is there a link between this new approach and the classical spectral stability theory?

The present study is a step towards answering the above points, which are discussed in the context of the linear stability of the Stuart vortices, which may be seen as a model of a mixing-layer with rolled-up Kelvin's 'cat's eyes', or as co-rotating vortices embedded in a background shear flow. Stuart's inviscid exact solution exhibits stagnation points with streamlines locally elliptical (in the cores) or hyperbolic (in the braids). In a non-rotating frame, the two- and three-dimensional stability of Stuart's vortices has been explored by Pierrehumbert & Widnall (1982) and Klaassen & Peltier (1989, 1991). In a rotating frame, Smyth & Peltier (1994, referred hereafter as SP94), examined the influence of the Coriolis force on the three-dimensional viscous instabilities of two-dimensional Kelvin–Helmholtz vortices, obtained by numerical simulations. They found that the influence of viscosity is weak, leading only to a cut-off for short-wavelength instability. Three kinds of modes have been brought to light in their work: the 'core', 'braid', and 'edge' modes. Their links with the present study will be discussed.

After a short review of the basic inviscid instability mechanisms in rotating fluids (§2), the rest of the paper is organized as follows: a description of the Stuart vortices is recalled in §3 and the governing equations are formulated in §4. The linear problem consists of non-parallel versions of the Orr–Sommerfeld and Squire equations, and a Floquet analysis (with respect to the streamwise space coordinate) is performed (§5). The resulting eigenvalue problem is solved by a spectral-collocation method, described in §6. Looking at the physics, the main tendencies of the Coriolis force are described in §7. In particular, the role of the hyperbolic and elliptical stagnation points is brought to light in §8, the core of the paper, and the spectral calculations are compared with the predictions of the geometrical optics stability theory. Finally, the effects of rapid rotation and propagation of inertial waves are discussed in §9.

2. Basic inviscid mechanisms

2.1. *Classical criteria*

In order to explain the effect of the Coriolis force on circular vortices, Kloosterziel (1990) extended the classical Rayleigh criterion for centrifugal instability to rotating fluids (see also Kloosterziel & van Heijst 1991; Mutabazi *et al.* 1992). This 'generalized' Rayleigh criterion states that *instability occurs when*

$$2(\Omega + V/r)(W + 2\Omega) < 0 \text{ somewhere,}$$

where $\boldsymbol{U}(r,\theta) = V(r)\boldsymbol{e}_\theta$ denotes the basic velocity field in a plane polar coordinate frame, and $W(r) = r^{-1}\mathrm{d}(rV)/\mathrm{d}r$ is the basic relative vorticity. As noted by LC97, this criterion states simply that *the flow is unstable if the square of the absolute circulation decreases somewhere*. In accordance with this criterion, the stabilizing and destabilizing effects of the Coriolis force on a circular monopolar vortex is clearly illustrated by Carnevale *et al.* (1997) with the Lamb vortex (Lamb 1932; Hopfinger & van Heijst

1993) characterized by a single-signed vorticity distribution $W(r) = -W_0 \exp(-r^2/2\delta^2)$ with W_0 and δ positive without lost of generality. Following the generalized Rayleigh criterion, instability occurs when $0 < 2\Omega < W_0$. Thus, *a weak anticyclonic rotation is destabilizing*, whereas other rotation rates are stabilizing (either cyclonic or stronger anticyclonic). This tendency was also observed for an isolated monopolar vortex (with zero net circulation) which is surrounded by a crown of vorticity of opposite sign, except that the unstable bandwidths may include the non-rotating case and weakly cyclonic rotations (Kloosterziel 1990; Hopfinger & van Heijst 1993). Identical mechanisms are observed in curved shear layers, and a review of the influence of rotation on Görtler instability may be found in Bottaro, Klingmann & Zebib (1996). This criterion has also been invoked by SP94 to explain the appearance of an 'edge' mode which destabilizes the row of Kelvin–Helmholtz rolls, for weak anticyclonic rotations.

This preliminary discussion gives a first indication of how to answer the second question which may be reformulated as: why don't strong anticyclonic vortices ever emerge? The answer could be: because they are linearly unstable. Indeed, for example, in a rotating fluid at given angular velocity (say Ω positive), a Lamb vortex with $W_0 > 2\Omega$ will be linearly unstable, whereas one with $W_0 \leqslant 2\Omega$ is possibly linearly stable. Obviously, the first case corresponds to a strong anticyclone (negative vorticity, positive rotation rate and $|W_0| > |2\Omega|$). The second case corresponds to weak anticyclones and cyclones (weak or strong). Of course, this is not new (Kloosterziel 1990; Kloosterziel & van Heijst 1991; SP94; Carnevale *et al.* 1997), but it illustrates the equivalence of the following statements: *strong anticyclones are unstable* and *a weak anticyclonic rotation is destabilizing*.

Exactly the same tendencies are observed for shear flows with parallel streamlines, e.g. $\boldsymbol{U}(x, y) = U(y)\boldsymbol{e}_x$, for which the classical 'Pedley' (or 'Bradshaw–Richardson–Tritton') criterion is applied. Derived rigorously by Pedley (1969), it states that *instability occurs when*

$$2\Omega(W + 2\Omega) < 0 \text{ somewhere,}$$

(with $W(y) = -\mathrm{d}U/\mathrm{d}y$ the basic vorticity) showing clearly that a single-signed vorticity shear flow such as the hyperbolic-tangent mixing layer with vorticity distribution $W(y) = -W_0 \cosh^{-2}(y/\delta)$ (W_0 and δ positive) is unstable when $0 < 2\Omega < W_0$ (Yanase *et al.* 1993). This is illustrated on figure 1. This criterion exhibits a strong similarity with the generalized Rayleigh criterion, except for the curvature term V/r.

Another inviscid exact instability criterion has been derived for the class of plane quadratic flows subjected to the Coriolis force (Craik 1989; Cambon *et al.* 1994). This class of solutions includes the unbounded elliptical vortex, the hyperbolic flow and the unbounded Couette-like (or pure-shear) flow. They are characterized by two parameters: the vorticity W and the strain rate D which are both uniform in the flow domain (with W and D positive). And *instability occurs if*

$$-\tfrac{1}{2}W - D < 2\Omega < -\tfrac{1}{2}W + D.$$

This is of course a sufficient condition for instability, since the well-known 'elliptical instability' occurs without rotation (Pierrehumbert 1986; Bayly 1986; Waleffe 1989, 1990), but is killed for 'zero absolute vorticity' $W + 2\Omega = 0$ (Craik 1989; Cambon *et al.* 1994; Bayly *et al.* 1996; Lebovitz & Lifschitz 1996).

2.2. *Pressureless modes and stagnation points*

These three stability criteria are characterized by the sign of the second invariant of the 'inertial tensor' and may be expressed jointly as (LC97): *a sufficient condition for*

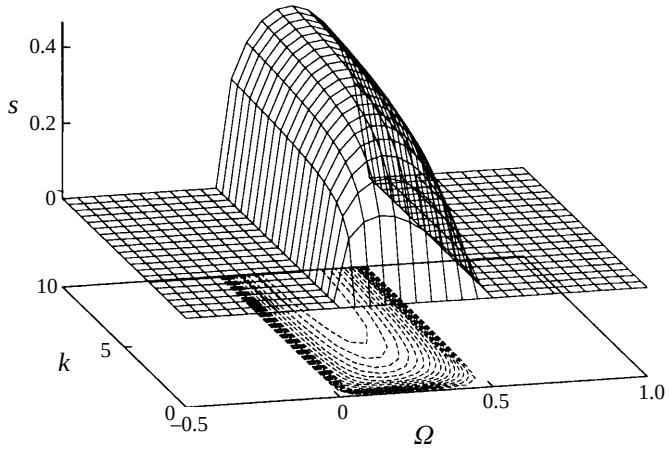

FIGURE 1. Growth rate of eigenmodes with $\alpha = 0$ for the mixing layer $U(y) = \tanh(y)$.

instability is that

$$-\tfrac{1}{2}\boldsymbol{S}:\boldsymbol{S} + \tfrac{1}{4}\boldsymbol{W}_t \cdot \boldsymbol{W}_t < 0 \text{ somewhere in the flow domain,}$$

where $\boldsymbol{W}_t$ and $\boldsymbol{S}$ are respectively the 'tilting vorticity' (Cambon *et al.* 1994) and the rate-of-strain tensor of the basic flow, expressed in Cartesian coordinates (x, y, z) (in curvilinear coordinates, a curvature term appears in the criterion). In agreement with Bayly (1988) for the centrifugal instability, LC97 showed that when instability occurs in accordance with this criterion, a class of three-dimensional 'pressureless' modes is excited. These modes are characterized by a wave vector perpendicular to the plane of the basic flow (or equivalently aligned with the rotation axis $\boldsymbol{k} = k\boldsymbol{e}_z$). When the physical problem exhibits a characteristic lengthscale L, they consist of short-wavelength ($k \gg L^{-1}$) eigenmodes strongly localized on streamlines. Otherwise, for quadratic flows (and no other examples are known), these pressureless modes are spatially uniform and not localized in the (x, y)-plane.

Figure 1 is an illustration of the tendencies described above. It corresponds to spectral stability calculations of the dimensionless mixing layer $U(y) = \tanh(y)$ (the numerical method is described later). The map represents the growth rate $s = \mathrm{Re}(\sigma)$ of the most unstable eigenmode $\boldsymbol{v}'(\boldsymbol{x}, t) = \mathrm{e}^{\sigma t}\mathrm{e}^{\mathrm{i}\alpha x}\mathrm{e}^{\mathrm{i}kz}\boldsymbol{v}(y)$ for a pure spanwise wave vector ($\alpha = 0$ and $k \neq 0$), as a function of the dimensionless rotation rate Ω. Illustrating the Pedley criterion (instability with $\alpha = 0$ occurs only if $0 < 2\Omega < 1$), it shows also that for increasing k (and fixed Ω), the growth rate $s = \mathrm{Re}(\sigma)$ of the eigenmodes asymptotes to a constant value, which in fact is predicted by the pressureless dynamics (LC97).

Recently, the Lifschitz & Hameiri (1991) theory for short-wave instability has been used to show that *any steady inviscid plane flow subjected (or not) to a Coriolis force is three-dimensionally unstable if*

$$\Phi(\boldsymbol{x}_0) = -\tfrac{1}{2}\boldsymbol{S}:\boldsymbol{S} + \tfrac{1}{4}\boldsymbol{W}_t \cdot \boldsymbol{W}_t < 0$$

on a stagnation point located at $\boldsymbol{x}_0$ (Leblanc 1997). Φ is the discriminant introduced in LC97. In fact, this powerful theory allows one to apply all the results obtained for the unrealistic quadratic flows reviewed above to the local topology of any complex basic flow. Thus, for example, the short-wave stability characteristics of an elliptical vortex core are analogous of the unbounded 'elliptical instability'. Bayly *et al.* (1996)

and Lebovitz & Lifschitz (1996) took advantage of this to study various complex flows. In particular, it could be shown (Cambon *et al.* 1994; Leblanc 1997) that at zero absolute vorticity

$$\boldsymbol{W}(\boldsymbol{x}_0) + 2\boldsymbol{\Omega} = 0,$$

any vortex core (locally circular or elliptical) and any pure-shear stagnation point (with locally parallel streamlines) is exponentially stable (the pure-shear case leads to an algebraic growth, damped by viscosity).

In view of all the results of this section, stabilization of vortices at zero absolute vorticity appears to be a generic feature of rotating flows. This is in contradiction with the heuristic criterion proposed by Lesieur, Yanase & Métais (1991), which predicts *"a catastrophic three-dimensional destabilization"* at zero-absolute vorticity (see discussions in Cambon *et al.* 1994). On the other hand, at zero tilting vorticity

$$\boldsymbol{W}(\boldsymbol{x}_0) + 4\boldsymbol{\Omega} = 0,$$

any stagnation point (except circular) is unstable.

3. Stuart's array of vortices

3.1. *Description*

It is well-known that a two-dimensional steady solution of the Euler equation described by the streamfunction Ψ satisfies

$$J(\Psi, \nabla^2\Psi) = 0,$$

with J the Jacobian operator, and then vorticity is constant along streamlines. This relation is satisfied if there exists an arbitrary function $\mathscr{F}$ such that $W = -\nabla^2\Psi = \mathscr{F}(\Psi)$.

Discovered by Stuart (1967), the dimensionless streamfunction

$$\Psi(x, y) = \log(\cosh y - \rho\cos x),\ 0 \leqslant \rho \leqslant 1 \tag{3.1}$$

is a solution of the Liouville equation $\nabla^2\Psi = (1-\rho^2)\exp(-2\Psi)$. This exact solution describes a shear layer centred on the x-axis between two uniform streams. Indeed $U \sim \pm 1$ and $V \sim 0$ when $y \to \pm\infty$. If $\rho = 0$, the hyperbolic-tangent mixing layer with parallel streamlines is recovered, whereas for $\rho = 1$, (3.1) describes a single row of co-rotating point vortices, with circulation -4π, periodically spaced along the x-axis (Lamb 1932). In the intermediate range ($0 < \rho < 1$), the shear layer exhibits two-dimensional co-rotating eddies with a smooth vorticity distribution, that resembles the Kelvin's 'cat's eyes' of critical layers (Drazin & Reid 1981). They are periodically spaced along the x-axis with period $l_x = 2\pi$, and as shown by Stuart (1967), their circulation is also -4π. For values of the shape parameter ρ between 0.2 and 0.6, the Stuart streamfunction resembles a two-dimensional mixing layer with rolled-up Kelvin–Helmholtz vortices, originated from primary instability of the $\tanh(y)$ parallel profile (Ho & Huerre 1984), even if, as mentioned by Stuart (1967), the streamwise wavenumber of the most unstable linear mode given by the temporal stability analysis of Michalke (1964) is $\alpha = 0.4446$, whereas $\alpha = 1$ (the wavenumber of the Stuart vortices) yields neutral modes. Another objection is that Stuart's streamfunction does not exhibit the viscous braids linking adjacent Kelvin–Helmholtz rolls, which break the $(x, y) \to (-x, -y)$ symmetry of (3.1). However, Stuart's solution is a convenient model for analytical studies.

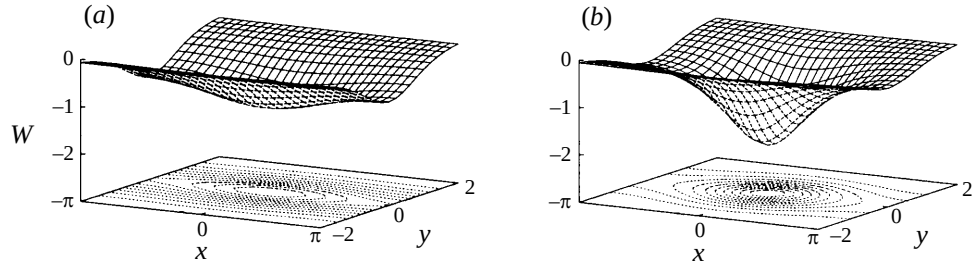

FIGURE 2. Vorticity and streamlines of Stuart's exact solution. (*a*) $\rho = 1/10$; (*b*) $\rho = 1/3$.

Its vorticity

$$W(x, y) = (\rho^2 - 1)/(\cosh y - \rho \cos x)^2$$

is everywhere negative. Far from the shear layer, the flow is irrotational. The vorticity in the cores located at $x = 2p\pi$ (p integer) is $(\rho + 1)/(\rho - 1)$; it increases with ρ in order to conserve the net circulation -4π. Most of the stability calculations have been performed with $\rho = 1/10$ and $\rho = 1/3$ for which the vorticity distribution is represented on figure 2. The streamlines of one period of the Stuart vortices on figure 2(*b*) are close to the trajectories measured in Jupiter's 'Great Red Spot', which is an isolated vortex in a shear flow (see figure 2 in Marcus 1993 or figure 1 in Dowling 1995). It is clear that this comparison is only qualitative because Jupiter's 'Great Red Spot' has a depth which is much smaller than its lateral extent. However, since the Coriolis force promotes short-wavelength instabilities, it is reasonable to suppose that they may be excited (or killed) in thin layers.

3.2. *Stagnation points*

In the vicinity of the vortex cores ($x = 2p\pi$, p integer), the Stuart streamfunction reads

$$\Psi_E \sim \tfrac{1}{2}(y^2 + \rho x^2)/(1 - \rho)$$

showing clearly that the streamlines are locally elliptical when $0 < \rho < 1$, whereas in the vicinity of the stagnation points located in the braids ($x = (2p + 1)\pi$, p integer), (3.1) behaves as

$$\Psi_H \sim \tfrac{1}{2}(y^2 - \rho x^2)/(1 + \rho)$$

exhibiting hyperbolic streamlines. On these stagnation points, the plane velocity gradient reads

$$\nabla \boldsymbol{U}_{E,H} = \begin{pmatrix} 0 & -\gamma - \epsilon \\ \gamma - \epsilon & 0 \end{pmatrix}, \tag{3.2}$$

with

$$\epsilon = -\tfrac{1}{2} \quad \text{and} \quad \gamma = \begin{cases} \tfrac{1}{2}(\rho + 1)/(\rho - 1) & \text{for elliptical cores } (|\gamma| > |\epsilon|), \\ \tfrac{1}{2}(\rho - 1)/(\rho + 1) & \text{for hyperbolic regions } (|\gamma| < |\epsilon|). \end{cases} \tag{3.3}$$

4. Governing equations

4.1. *Equations of motion*

In a frame rotating at a constant angular velocity $\boldsymbol{\Omega}$, the relative motion of an incompressible inviscid fluid is governed by Euler and continuity equations, that read

in non-dimensional form, and without any non-conservative body forces other than the Coriolis force

$$\partial_t \boldsymbol{u} + \boldsymbol{u} \cdot \nabla \boldsymbol{u} + 2\boldsymbol{\Omega} \times \boldsymbol{u} = -\nabla \pi, \ \nabla \cdot \boldsymbol{u} = 0. \tag{4.1}$$

The relative velocity $\boldsymbol{u}(\boldsymbol{x}, t)$ has been non-dimensionalized by a characteristic velocity scale U, the position vector $\boldsymbol{x}$ by a characteristic lengthscale L, and time t by L/U. The coordinate frame rotates at the non-dimensional angular velocity $\boldsymbol{\Omega}$, which has also been non-dimensionalized by L/U, such that $|\boldsymbol{\Omega}|$ may be seen as the inverse of a global Rossby number; $\pi(\boldsymbol{x}, t)$ is the non-dimensional modified pressure field including the contributions of the centrifugal force and other conservative body forces applied to the fluid.

If the relative motion of the flow is purely two-dimensional in the plane perpendicular to the axis of rotation, say $\boldsymbol{e}_z$, then the Coriolis force is conservative since $2\boldsymbol{\Omega} \times \boldsymbol{u} = \nabla(2\Omega\psi)$, where $\psi(x, y, t)$ is the two-dimensional streamfunction. Thus, for an observer moving with the rotating frame, the flow motion is not affected by the Coriolis force. This property is very important because it allows one to choose any two-dimensional flow motion in the (x, y)-plane as basic states for the stability analysis in the rotating frame. Another consequence is that the Coriolis force acts only on three-dimensional perturbations, whereas two-dimensional perturbations are unaffected.

4.2. *Linear problem*

In a Cartesian coordinate frame $(\boldsymbol{e}_x, \boldsymbol{e}_y, \boldsymbol{e}_z)$ rotating with angular velocity vector $\boldsymbol{\Omega} = \Omega \boldsymbol{e}_z$, let $\boldsymbol{U}(x, y) = (U(x, y), V(x, y), 0)$ and $\Pi(x, y)$ describe the relative motion of a two-dimensional steady flow. Adding a three-dimensional perturbation $\boldsymbol{u}'(\boldsymbol{x}, t)$ and $\pi'(\boldsymbol{x}, t)$, substituting into (4.1) and neglecting quadratic terms, the linearized equations read, following LC97,

$$\mathrm{D}_t \boldsymbol{u}' + \boldsymbol{S}\,\boldsymbol{u}' + \tfrac{1}{2}\boldsymbol{W}_t \times \boldsymbol{u}' = -\nabla \pi', \quad \nabla \cdot \boldsymbol{u}' = 0, \tag{4.2}$$

where $\mathrm{D}_t = \partial_t + \boldsymbol{U} \cdot \nabla$ is the material derivative following the basic flow, $\boldsymbol{S} = \frac{1}{2}(\nabla \boldsymbol{U} + \nabla \boldsymbol{U}^T)$ is the basic rate-of-strain tensor of the basic flow, and $\boldsymbol{W}_t = \boldsymbol{W} + 4\boldsymbol{\Omega}$ is the 'tilting vorticity' of the basic flow (Cambon *et al.* 1994).

No coefficient of the linear problem involves a z-dependence; it is thus possible to Fourier transform in the $\boldsymbol{e}_z$-direction, or equivalently to seek perturbations of the following form:

$$[\boldsymbol{u}', \pi'](\boldsymbol{x}, t) = \mathrm{e}^{\mathrm{i}kz}[\boldsymbol{u}, \pi](x, y, t),$$

where the spanwise wavenumber k is real to ensure homogeneity of the solution when $z \to \pm\infty$. Without specifying the basic flow and boundary conditions, nothing can be said about $[\boldsymbol{u}, \pi](x, y, t)$. Equation (4.2) reads

$$\mathrm{D}_t \boldsymbol{v} + \boldsymbol{M}\,\boldsymbol{v} = -\nabla \pi, \quad \mathrm{D}_t w = -\mathrm{i}k\pi, \quad \nabla \cdot \boldsymbol{v} + \mathrm{i}kw = 0; \tag{4.3}$$

$\boldsymbol{v}(x, y, t)$ is the projection of $\boldsymbol{u}(x, y, t)$ on the (x, y)-plane, whereas $w(x, y, t)$ is its spanwise component. $\nabla(\ )$ and $\nabla \cdot (\ )$ are now the gradient and divergence operator in the (x, y)-plane. The 2×2 'inertial tensor' $\boldsymbol{M}$ is defined by

$$\boldsymbol{M} = \boldsymbol{N} + \boldsymbol{C} \quad \text{with} \quad \boldsymbol{C} = \begin{pmatrix} 0 & -2\Omega \\ 2\Omega & 0 \end{pmatrix}, \tag{4.4}$$

where $\boldsymbol{N} = \nabla \boldsymbol{U}$, $\boldsymbol{C}$ is the 'Coriolis tensor', and in a curvilinear plane coordinate frame, $\boldsymbol{M}$ involves an additional antisymmetric 'curvature tensor' (LC97). The two

eigenvalues of $\boldsymbol{M}$ are solutions of the characteristic equation

$$\lambda^2 + \Phi = 0 \quad \text{where} \quad \Phi = -\tfrac{1}{2}\boldsymbol{M}:\boldsymbol{M} = -\tfrac{1}{2}\mathrm{tr}\boldsymbol{M}^2$$

is the second invariant of the inertial tensor $\boldsymbol{M}$. In Cartesian coordinates, this 'general discriminant' reads (LC97)

$$\begin{aligned}\Phi(x,y) &= -\tfrac{1}{2}\boldsymbol{S}:\boldsymbol{S} + \tfrac{1}{4}\boldsymbol{W}_t \cdot \boldsymbol{W}_t \\ &= (\Psi_{xx} - 2\Omega)(\Psi_{yy} - 2\Omega) - (\Psi_{xy})^2, \end{aligned} \tag{4.5}$$

where $\Psi(x,y)$ is the basic streamfunction and the subscripts denote partial differentiation.

Considering the structure of the linear problem (4.3) and the expression for the inertial tensor (4.4), the Coriolis force acts on instabilities as a tuner of their non-rotating counterparts. This idea is clearly illustrated for quadratic flows and the 'elliptical instability' (Craik 1989; Cambon *et al.* 1994). Indeed, the stabilizing or destabilizing influence of rotation is described by the shift of the angular band of unstable oblique (and time-dependent) wave vectors (see figure 4 in Cambon *et al.* 1994).

4.3. *Non-parallel Orr–Sommerfeld and Squire equations*

Without solid-body rotation, three-dimensional stability analyses of basic flows with non-parallel streamlines require solving the linear system composed of non-parallel versions of the Orr–Sommerfeld and Squire equations (Orszag & Patera 1981, 1983; Herbert, Bertolotti & Santos 1987). The Coriolis force may be added without major difficulty.

In the following, the partial spatial derivatives of the streamfunction and vorticity of the basic flow are denoted with a subscript. Thus the basic vorticity reads $W = -(\Psi_{xx} + \Psi_{yy})$. The partial derivative operators applied to the velocity perturbation are denoted for example by $\partial_{xy} = \partial^2/\partial x \partial y$. The material derivative following the basic flow now reads $\mathrm{D}_t = \partial_t + \Psi_y \partial_x - \Psi_x \partial_y$. The non-parallel Orr–Sommerfeld equation is obtained by applying the Laplacian operator to the second component of the linearized Euler equation. Pressure is easily eliminated using the linearization of the Poisson equation. After some manipulations and tedious algebra, one obtains

$$\begin{aligned}&(\mathrm{D}_t - \Psi_{xy})(\partial_{xx} + \partial_{yy} - k^2)v \\ &\quad = (-2W_x\partial_x + 2\Psi_{xy}\partial_{xy} - W_{xx} + (\Psi_{xx} - 2\Omega)(\partial_{xx} - k^2) - \Psi_{xx}\partial_{yy})u \\ &\qquad +(-W_x\partial_y - W_y\partial_x - W_{xy} - 2\Psi_{xy}\partial_{xx} + 2(\Psi_{xx} - \Omega)\partial_{xy})v, \end{aligned} \tag{4.6}$$

where u and v are the components of the velocity perturbation in the plane of the basic flow. The non-parallel Squire equation is the second component of the linearized Helmholtz equation for the vorticity perturbation $\boldsymbol{\omega}(x,y,t) = \nabla \times \boldsymbol{u} = (\xi, \eta, \zeta)$:

$$(\mathrm{D}_t + \Psi_{xy})\eta + \Psi_{xx}\xi = \mathrm{i}k(W + 2\Omega)v, \tag{4.7}$$

which may be expressed exclusively as a function of u and v, using the relations $\mathrm{i}k\eta = (\partial_{xx} - k^2)u + \partial_{xy}v$ and $\mathrm{i}k\xi = -\partial_{xy}u - (\partial_{yy} - k^2)v$ obtained taking into account the incompressibility constraint.

Viscosity may be easily taken into account by replacing D_t by $\mathrm{D}_t - \nu(\partial_{xx} + \partial_{yy} - k^2)$ in the left-hand side of (4.6) and (4.7). This is the reason why the terminology 'Orr–Sommerfeld' and 'Squire' equations has been used. SP94 have solved the viscous problem with an alternative formulation, and Klaassen & Peltier (1985, 1989, 1991) included the effects of stratification. For basic flows with parallel streamlines, (4.6)

and (4.7) reduce to the classical Orr–Sommerfeld and Squire equations that are not decoupled owing to the Coriolis force. Furthermore, Squire's theorem does not hold, as mentioned by Yanase *et al.* (1993). And finally, in the context of Görtler instability with system rotation and for a spatially varying basic flow, an equivalent formulation is given by Bottaro *et al.* (1996).

5. Eigenvalue problem

5.1. *Floquet analysis*

The linear system composed of (4.6) and (4.7) for $\boldsymbol{v} = (u, v)$ may be written

$$\partial_t \mathscr{L}_1 \boldsymbol{v}(x, y, t) = \mathscr{L}_2 \boldsymbol{v}(x, y, t) \tag{5.1}$$

where $\mathscr{L}_i = \mathscr{L}_i(\Psi; \Omega, k)$ for $i = 1, 2$ are linear operators involving the partial derivatives of the streamfunction and the square of the spanwise wavenumber of the perturbation. It is then sufficient to consider

$$k \geqslant 0.$$

In fact this may be directly concluded from (4.3), which is invariant under the transformation $(k, w) \rightarrow (-k, -w)$.

For spatially periodic basic flows, with period $l_x = 2\pi/\alpha$, (5.1) involves l_x-periodic coefficients, and Floquet theory (Kelly 1967; Herbert 1983, 1988; Klaassen & Peltier 1985, 1989, 1991) allows one to seek perturbations of the form

$$\boldsymbol{v}(x, y, t) = \mathrm{e}^{\sigma t} \mathrm{e}^{\mathrm{i}\mu x} \tilde{\boldsymbol{v}}(x, y) \tag{5.2}$$

where the complex number $\mu' = \mathrm{i}\mu$ is a Floquet exponent, and $\tilde{\boldsymbol{v}}(x, y)$ are l_x-periodic like the basic flow ($l_x = 2\pi$ for the Stuart vortices). In order to perform a temporal stability analysis (σ complex), the Floquet exponent μ' is purely imaginary and μ is now a (real) parameter of the problem (a spatial stability analysis requires σ imaginary and μ complex). According to Herbert (1988), it is easy to check that Floquet modes (5.2) are invariant under the transformation $\mu \rightarrow \mu \pm p\alpha$, with p integer, because $\exp(\pm \mathrm{i}p\alpha x)\tilde{\boldsymbol{v}}(x, y)$ is invariant under the translation $x \rightarrow x \pm l_x$. Therefore, it is sufficient to consider $-\alpha/2 < \mu \leqslant \alpha/2$. Klaassen & Peltier (1989) have provided a detailed discussion of the symmetries involved in the Floquet modes for the stratified free shear layer.

5.2. *Fundamental and subharmonic modes*

Since the product of two periodic functions is periodic if the ratio of the periods is a rational number, the Floquet mode (5.2) is periodic if $|\mu/\alpha| = m/n$, with m and n integer numbers. Recalling that $\alpha = 2\pi/l_x$ is the wavenumber of the basic flow and that $-1/2 < \mu/\alpha \leqslant 1/2$, there are two main classes of modes, according to Herbert (1988).

The *fundamental* modes ($\mu/\alpha = 0$) are l_x-periodic like the basic flow. Physically, without the Coriolis force, they tend to deform in phase spatially and three-dimensionally (with spanwise wavenumber k) the structure of the basic flow: they correspond to aligned 'Λ-patterns' observed in boundary-layers (Herbert 1983, 1988) and to 'translative' instabilities observed in mixing layers (Pierrehumbert & Widnall 1982; Metcalfe *et al.* 1987).

The *subharmonic* modes ($\mu/\alpha = 1/2$) have twice the periodicity of the basic flow. For non-rotating shear flows, these $2l_x$-periodic modes excite the staggered 'Λ-patterns' of

boundary layers (Herbert 1983, 1988), and for mixing layers with rolled-up Kelvin–Helmholtz vortices (in fact the Stuart streamfunction) Pierrehumbert & Widnall (1982) showed that the subharmonic modes excite the 'helical pairing' of two adjacent vortices.

According to Herbert (1983, 1988), fundamental modes are associated with primary resonance in the Floquet system, and subharmonic ones with the principal parametric resonance. Other classes of modes in the range $0 < |\mu/\alpha| < 1/2$ exist ('detuned' following the terminology of Herbert 1988), periodic if μ/α is rational or aperiodic otherwise. For purely two-dimensional perturbation ($k = 0$), Pierrehumbert & Widnall (1982) showed that fundamental modes of Stuart vortices are neutral, whereas subharmonic are amplified. Klaassen & Peltier (1989) showed that the most unstable two-dimensional modes are the pairing ones ($\mu/\alpha = 1/2$), and they also showed that modes such that $|\mu/\alpha| = 1/n$, with $n > 2$, tend to amalgamate more than two adjacent vortices, but are less amplified than subharmonic modes. This is of course consistent with experimental observations and numerical simulations showing frequent pairings. This is also consistent with Lamb's linear stability analysis of the array of periodically spaced co-rotating point vortices (Lamb 1932), where the most unstable modes are subharmonic.

5.3. *Symmetries and spectrum*

With (5.2), the eigensystem (5.1) becomes

$$\sigma \mathscr{L}_1 \tilde{\boldsymbol{v}}(x, y) = \mathscr{L}_2 \tilde{\boldsymbol{v}}(x, y) \tag{5.3}$$

with now $\mathscr{L}_i = \mathscr{L}_i(\Psi\,; \Omega, k, \mu)$ for $i = 1, 2$. Thus, given a basic flow and the parameters (Ω, k, μ), the problem consists in seeking eigenmodes $(\sigma, \tilde{\boldsymbol{v}})$ of (5.3) such as $\tilde{\boldsymbol{v}}(x, y)$, l_x-periodic, vanishes when $y \to \pm\infty$. The system is composed of the non-parallel Orr–Sommerfeld and Squire equations (4.6) and (4.7) which read now respectively

$$\begin{aligned}
\sigma(\tilde{\partial}_{xx} + \partial_{yy} - k^2)\tilde{v} = {} & (-2W_x\tilde{\partial}_x + 2\Psi_{xy}\tilde{\partial}_{xy} - W_{xx} + (\Psi_{xx} - 2\Omega)(\tilde{\partial}_{xx} - k^2) - \Psi_{xx}\partial_{yy})\tilde{u} \\
& + (-W_x\partial_y - W_y\tilde{\partial}_x - W_{xy} - 2\Psi_{xy}\tilde{\partial}_{xx} + 2(\Psi_{xx} - \Omega)\tilde{\partial}_{xy} \\
& - (\Psi_y\tilde{\partial}_x - \Psi_x\partial_y - \Psi_{xy})(\tilde{\partial}_{xx} + \partial_{yy} - k^2))\tilde{v}, \\
\sigma((\tilde{\partial}_{xx} - k^2)\tilde{u} + \tilde{\partial}_{xy}\tilde{v}) = {} & (\Psi_{xx}\tilde{\partial}_{xy} - (\Psi_y\tilde{\partial}_x - \Psi_x\partial_y + \Psi_{xy})(\tilde{\partial}_{xx} - k^2))\tilde{u} \\
& + (\Psi_{xx}\partial_{yy} - k^2(2\Omega - \Psi_{yy}) - (\Psi_y\tilde{\partial}_x - \Psi_x\partial_y + \Psi_{xy})\tilde{\partial}_{xy})\tilde{v},
\end{aligned}$$

where $\tilde{\partial}_x = \mathrm{i}\mu + \partial_x$, $\tilde{\partial}_{xx} = (\mathrm{i}\mu + \partial_x)^2$ and $\tilde{\partial}_{xy} = (\mathrm{i}\mu + \partial_x)\partial_y$. Taking the complex conjugate of (5.3), it is easy to check that $(\sigma^*, \tilde{\boldsymbol{v}}^*)$ is an eigenmode for $(\Omega, k, -\mu)$, exhibiting the same growth rate $s = \mathrm{Re}(\sigma)$ as that of the mode $(\sigma, \tilde{\boldsymbol{v}})$. Then it is sufficient to consider μ positive, and thus, taking into account previous considerations,

$$0 \leqslant \mu \leqslant \alpha/2.$$

As for the non-rotating case (Pierrehumbert & Widnall 1982), it may be shown that the spectrum of eigenvalues associated to the given parameters (Ω, k, μ) contains $\pm\sigma$ and $\pm\sigma^*$. Let $(\sigma, \tilde{u}, \tilde{v})$ be a Floquet mode of (5.3) for the parameters (Ω, k, μ). Indeed, applying first the transformation $y \to -y$ in (5.3), and taking into account the symmetries of the Stuart streamfunction (3.1) and its derivative, it is easy to verify that $(-\sigma, -\tilde{u}, \tilde{v})$ is an eigenmode for the same set of parameters. It means that the eigenvalue spectrum contains σ and $-\sigma$; the immediate consequence is that for each unstable mode there is a corresponding stable mode, and then *the basic flow is at best neutrally stable*. As already mentioned by Pierrehumbert & Widnall (1982)

for the non-rotating case, this is a manifestation of the time-reversibility of Euler equations and does not hold with viscosity: with $t \to -t$ it is always possible to find an additional transformation leaving the Euler equations invariant. Now taking the complex conjugate of (5.3) and applying $x \to -x$, it is easy to check that $(\sigma^*, \tilde{u}^*, -\tilde{v}^*)$ is also an eigenmode for the parameters (Ω, k, μ). It follows immediately that $-\sigma^*$ belongs as well to the eigenvalue spectrum associated with these parameters. Thus, in the complex map, the spectrum contains $\pm\sigma$ and $\pm\sigma^*$.

6. Spectral resolution

6.1. *Fourier–Chebyshev series*

In order to transform the infinite interval $y \in]-\infty;+\infty[$ to the finite one $Y \in]-1;+1[$, the exponential mapping (Metcalfe *et al.* 1987)

$$Y = \tanh(y/H)$$

has been used. The l_x-periodic eigenfunctions may then be expanded in the double infinite series

$$\tilde{\boldsymbol{v}}(x, y) = \sum_{m=-\infty}^{+\infty} \sum_{n=0}^{+\infty} \tilde{\boldsymbol{v}}_{m,n} \mathrm{e}^{\mathrm{i}\alpha m x} T_n(Y), \tag{6.1}$$

where the Chebyshev polynomials $T_n(Y) = \cos(n\theta)$ with $\theta = \arccos Y$ and $\theta \in]0;\pi[$, satisfy naturally the boundary conditions when $Y \to \pm 1$ (Canuto *et al.* 1988).

6.2. *Truncations*

The truncation of the series must take into account certain relations between the unknown coefficients $\tilde{\boldsymbol{v}}_{mn} = (\tilde{u}_{m,n}, \tilde{v}_{m,n})$, in order to respect symmetries of the Stuart streamfunction and its derivative. Indeed, Klaassen & Peltier (1989) have shown by symmetry considerations that

$$\tilde{\boldsymbol{v}}_{m,n} = \pm(-1)^n \tilde{\boldsymbol{v}}_{-(m+2\mu/\alpha),n}, \tag{6.2}$$

a relation satisfied only if $m + 2\mu/\alpha$ is integer. Thus, for the fundamental modes ($\mu/\alpha = 0$), the truncation must retain coefficients with $m = m_0$ and $m = -m_0$ in order to satisfy $\tilde{\boldsymbol{v}}_{m,n} = \pm(-1)^n \tilde{\boldsymbol{v}}_{-m,n}$. Then, for fundamental modes, a possible truncated expansion is

$$\tilde{\boldsymbol{v}}(x, y) = \sum_{m=-M'}^{M'} \sum_{n=0}^{N-1} \tilde{\boldsymbol{v}}_{m,n} \mathrm{e}^{\mathrm{i}\alpha m x} \cos(n\theta), \quad M' = (M-1)/2 \ \text{ with } M \text{ even}.$$

From (6.2), in the case of subharmonic modes ($\mu/\alpha = 1/2$), the coefficients verify $\tilde{\boldsymbol{v}}_{m,n} = \pm(-1)^n \tilde{\boldsymbol{v}}_{-m-1,n}$. In order to conserve the symmetries of Stuart flow, coefficients with $m = m_0$ and $m = -m_0 - 1$ have to appear in the expansion (6.1), which is satisfied with:

$$\tilde{\boldsymbol{v}}(x, y) = \sum_{m=-M'}^{M'-1} \sum_{n=0}^{N-1} \tilde{\boldsymbol{v}}_{m,n} \mathrm{e}^{\mathrm{i}\alpha m x} \cos(n\theta), \quad M' = M/2 \ \text{ with } M \text{ odd}.$$

Klaassen & Peltier (1989) have shown that violations of these requirements may lead to erroneous results. In fact, it may be verified that these different truncations for fundamental and subharmonic modes are equivalent to those used by Herbert (1983, 1988).

For basic flows with parallel streamlines, such as for example the hyperbolic-tangent

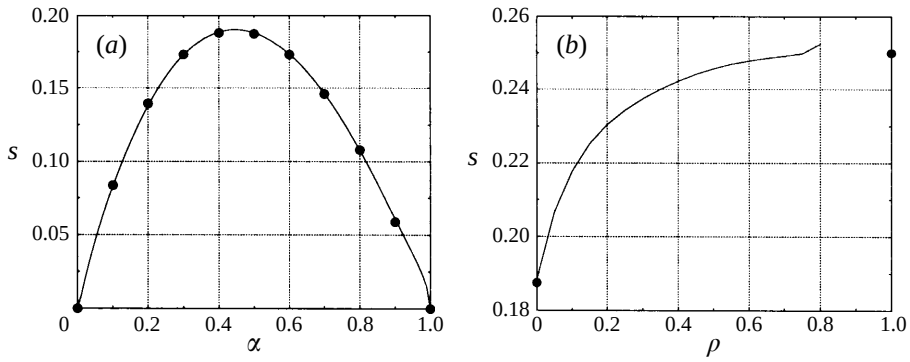

FIGURE 3. Two-dimensional stability calculations ($k = 0$) and comparison with data from Michalke (1964) (•). (*a*) Mixing layer for various streamwise wavenumbers α; (*b*) subharmonic modes of the Stuart vortices (the • at $\rho = 1$ corresponds to the point vortex case, Lamb 1932).

mixing layer $U(y) = \tanh(y)$ (Stuart's streamfunction with $\rho = 0$), it is possible to seek eigenmodes of the form $\boldsymbol{v}'(\boldsymbol{x}, t) = \mathrm{e}^{\sigma t}\mathrm{e}^{\mathrm{i}\alpha x}\mathrm{e}^{\mathrm{i}kz}\boldsymbol{v}(y)$ (α real), and to expand $\boldsymbol{v}(y)$ with Chebyshev polynomials using the same mapping.

6.3. *Collocation points*

To achieve the discretization of the continuous problem, we choose the collocation method instead of the Galerkin method for its simplicity of programming. The following collocation points are chosen:

$$x_j = 2\pi j/M,\ j = 0, \cdots, M-1 \quad \text{and} \quad \theta_k = (2k+1)\pi/(2N),\ k = 0, \cdots, N-1$$

in order to avoid the singular limits $y \to -\infty$ ($\theta \to \pi^-$) and $y \to +\infty$ ($\theta \to 0^+$). Thus the problem consists now in seeking the eigenvalues of the $(2MN)^2$-matrix problem $\sigma L_1 V = L_2 V$, with the eigenvectors $V = (\tilde{u}_{m,n}, \tilde{v}_{m,n})$. The complex matrix eigenvalue problem is solved by a standard QZ algorithm, which computes the $2MN$ eigenvalues of the discrete spectrum, and the associate eigenvectors.

The numerical parameters (H, M and N) are chosen in order to obtain good agreement with known results, such as for example the temporal stability analysis of the parallel tanh-mixing layer (Michalke 1964) plotted on figure 3(*a*). Two-dimensional stability calculations of the Stuart vortices are plotted on figure 3(*b*). For $\rho = 0$, the growth rate corresponds to Michalke's results (1964) for $\alpha = 1/2$, and it shows that results are erroneous when one reaches the singular point-vortex limit ($\rho \to 1$) for which the temporal growth rate of the subharmonic instability is $s = 1/4$ (Lamb 1932). The shape of the curve is similar to previous results (Pierrehumbert & Widnall 1982; Klaassen & Peltier 1989).

Another convenient way to test the numerical method is to solve $\sigma\tilde{\boldsymbol{v}}(x, y) = \boldsymbol{M}\tilde{\boldsymbol{v}}(x, y)$ and compare with the exact eigenvalues $\lambda = \pm(-\Phi)^{1/2}$ of the inertial tensor (4.4), with Φ given by (4.5). A good compromise has been found with $H = 0.7$, $M = 9$ (resp. $M = 10$) Fourier coefficients and $N = 16$ (resp. $N = 15$) Chebyshev polynomials for the fundamental (resp. subharmonic) Floquet modes.

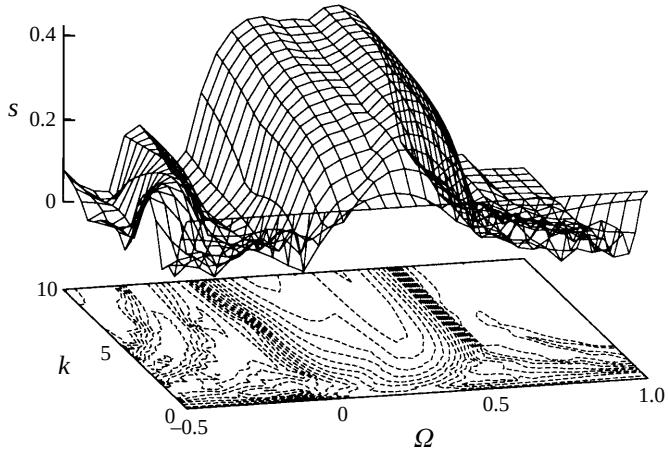

FIGURE 4. Growth rate of the subharmonic modes of the Stuart vortices with $\rho = 1/3$.

7. Global tendencies

7.1. *Stabilizing and destabilizing rotations*

Because the vorticity distribution of Stuart vortices is everywhere negative, $\Omega < 0$ corresponds to a cyclonic rotation, whereas $\Omega > 0$ corresponds to an anticyclonic one. Figure 4 is representative of the important role of the Coriolis force in the linear stability of Stuart vortices. This map represents the growth rate of the most unstable subharmonic mode as a function of the spanwise wavenumber k and of the rotation rate Ω, for $\rho = 1/3$ in (3.1). For $k = 0$, pairing modes are amplified with a growth rate $s = 0.239$ consistent with previous results (Pierrehumbert & Widnall 1982; Klaassen & Peltier 1989), whatever the background rotation since two-dimensional perturbations are unaffected. As soon as k grows, the influence of the Coriolis force on three-dimensional perturbations becomes apparent: a strong peak of instability is observed for weak anticyclonic rotations whereas stronger positive rotation rates tend to stabilize the basic flow by a cut-off effect. Similar results were obtained by SP94 for the viscous Kelvin–Helmholtz rolls under the effect of rotation. Thus, for $\Omega = 1$, only long-wavelength perturbations are amplified, whereas above a critical spanwise wavenumber ($k \approx 1$), three-dimensional short-wave perturbations are neutral. Qualitatively the same short-wave cut-off happens for cyclonic rotations, except that a little hump of instability tends to catch hold of the larger unstable band for large wavenumbers.

Looking at the isolevels on the base of figure 4, the growth rate tends to asymptote to a constant value for growing k. The same qualitative tendencies have been found for the fundamental Floquet modes (Leblanc & Cambon 1996), except for long-wave three-dimensional perturbations ($k \approx 0$), which are neutral at vanishing k (Pierrehumbert & Widnall 1982). Furthermore, for large k, fundamental and subharmonic modes were found to behave identically, even for the non-rotating case. This result is partially in contradiction with eigenvalue calculations by Pierrehumbert & Widnall (1982) who found that three-dimensional fundamental modes are unstable with a growth rate reaching a constant value at large wavenumber, whereas the subharmonic 'helical pairing' modes become neutral above a spanwise cut-off, contrary to the present results. This will be discussed later.

Temporal stability calculations are in qualitative agreement with experimental ob-

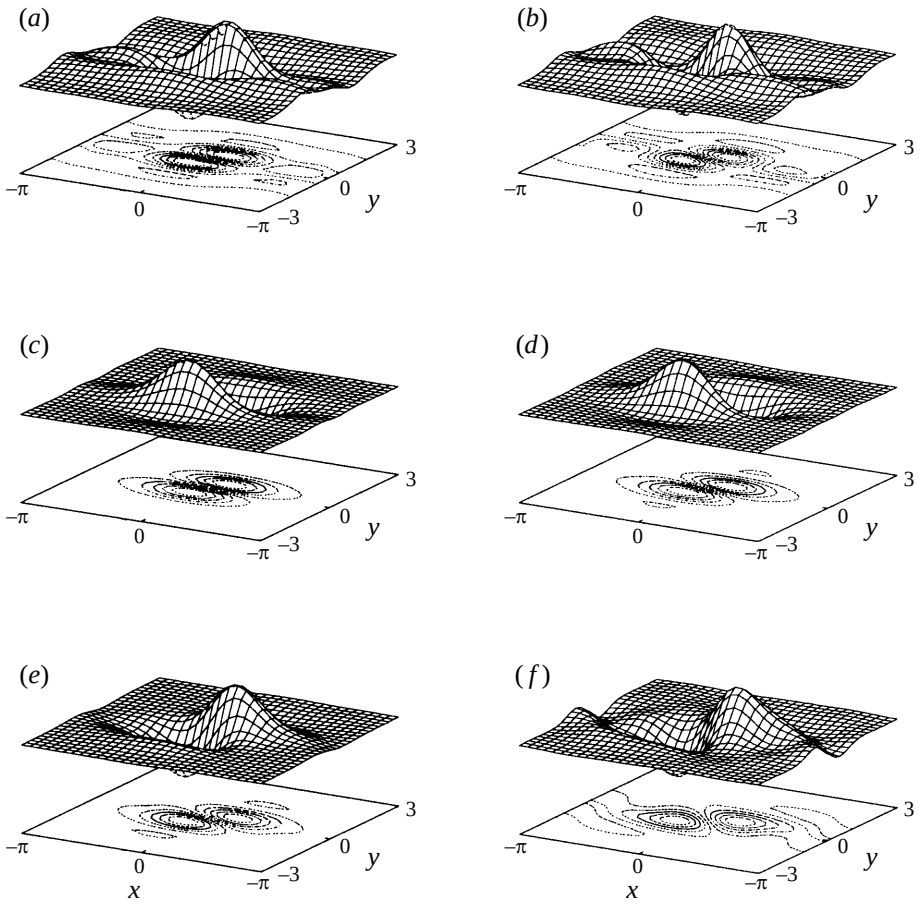

FIGURE 5. Spanwise vorticity of the fundamental modes for $k = 2$ and $\rho = 1/3$. (*a*) $\Omega = 0$; (*b*) $\Omega = 0.1$; (*c*) $\Omega = 0.2$; (*d*) $\Omega = 0.3$; (*e*) $\Omega = 0.4$; (*f*) $\Omega = 0.5$.

servations by Bidokhti & Tritton (1992) on a spatially developing turbulent mixing layer: *"the roller eddy pattern, familiar in non-rotating flow, was observed in all stabilized flow, but was almost completely disrupted by even weak destabilization"*. These tendencies are also in agreement with viscous stability calculations by SP94.

7.2. *Localized eigenmodes*

The Coriolis force alters considerablely the shape of the Floquet modes. Even if the instabilities are three-dimensional, the spanwise component of the perturbation of vorticity

$$\zeta(x, y, t) = \mathrm{e}^{\sigma t}\mathrm{e}^{\mathrm{i}\mu x}(\tilde{\partial}_x \tilde{v} - \partial_y \tilde{u})$$

gives useful information. On figure 5 is plotted the most unstable fundamental mode ($\mu = 0$) for various anticyclonic rotations in the unstable range, and for a moderate spanwise wavenumber ($k = 2$). Recall that they are 2π-periodic like the Stuart vortices; the nature of the instability changes with rotation, as pointed out firstly by SP94.

The following discussion is qualitative, and concerns only a particular value of the wavenumber k. As a consequence, this is not a 'zoological' classification of the different eigenmodes that could be obtained for all values of the control parameters of

the problem (Ω, k, μ). However, the instabilities described below seem representative of the short-wave behaviour of the eigenmodes ($k \to \infty$), on which most of the present study is focused.

In the non-rotating case (figure 5*a*), the fundamental eigenmode has a complex structure: it exhibits a dipole structure in the elliptical core of the vortices and extends into the braid region. Near the core, the topology of the eigenmode is close to that of the 'elliptical instability' (Pierrehumbert 1986; Waleffe 1989, 1990). In the hyperbolic regions, the structure of the eigenmode could correspond to the streamwise ribs linking adjacent vortices in rolled-up mixing layers (Ho & Huerre 1984; Metcalfe *et al.* 1987; Lasheras & Choi 1988), and to the 'braid' mode of SP94. For weak anticyclonic rotation (figure 5*b*), the eigenmode exhibits a similar shape. In these two cases, which correspond to a moderate spanwise wavenumber ($k = 2$), the topology of the modes suggests the coexistence of both elliptical and hyperbolic instabilities.

In the non-rotating case, for Stuart vortices, Klaassen & Peltier (1991) identified only a mode centred *"near the braid stagnation points"* (see their figure 26), but for the highest value of the spanwise wavenumber ($k = 5$). However they did not connect it to the 'hyperbolic instability' of the corresponding quadratic flow, to which tends asymptotically the growth rate of the most unstable eigenmode of Stuart's vortices when $k \to \infty$ (see further discussions), clearly in accordance with their observations.

For moderate rotation rates (figure 5*c*, *d*), the eigenmodes become localized into the vortex cores, and exhibit a shape close to the elliptical instability in an inertial frame (Pierrehumbert 1986; Waleffe 1989, 1990). SP94 observed similar behaviour with the viscous linear modes of the nonlinearly saturated Kelvin–Helmholtz vortices (the 'core' mode). Stronger anticyclonic rotations (figure 5*e*, *f*) modify the topology of the eigenmodes, and seem to tilt the structure of the elliptical instability.

Finally, the 'edge' mode discovered by SP94, which is focused into a ring-shaped region surrounding the central vortex, and explained by the generalized Rayleigh criterion of Kloosterziel & van Heijst (1991), has not been recovered in the present study. A possible explanation could be that the rolled-up Kelvin–Helmholtz vortices, which are the basic states in SP94, exhibit elliptical cores with weaker ellipticity than in our stability calculations. Thus, if the vortices are nearly circular, it seems reasonable to explain these 'edge' modes by the generalized Rayleigh criterion (SP94). This criterion predicts instability at a given radius, and then is localized on the corresponding streamline (LC97). The reason why the present study does not explore the weak ellipticity regime ($\rho \to 1$) is that Stuart's streamfunction becomes singular (array of point vortices), and requires a more accurate resolution.

8. Short-wave breakdown

8.1. *Pressureless eigenmodes*

In accordance with Bayly (1988) and several works on turbulence modelling (see Cambon *et al.* 1985, 1994; and references therein), LC97 showed that the Coriolis force promotes 'pressureless' modes. Indeed, formally speaking, the linear problem (4.3) can also be written:

$$\mathrm{D}_t \boldsymbol{v} + \boldsymbol{M}\,\boldsymbol{v} = 1/k^2(\nabla \mathrm{D}_t \nabla \cdot \boldsymbol{v}). \tag{8.1}$$

If the right-hand side vanishes, the 'pressureless' dynamics are governed by

$$\mathrm{D}_t \boldsymbol{v} + \boldsymbol{M}\,\boldsymbol{v} = 0, \tag{8.2}$$

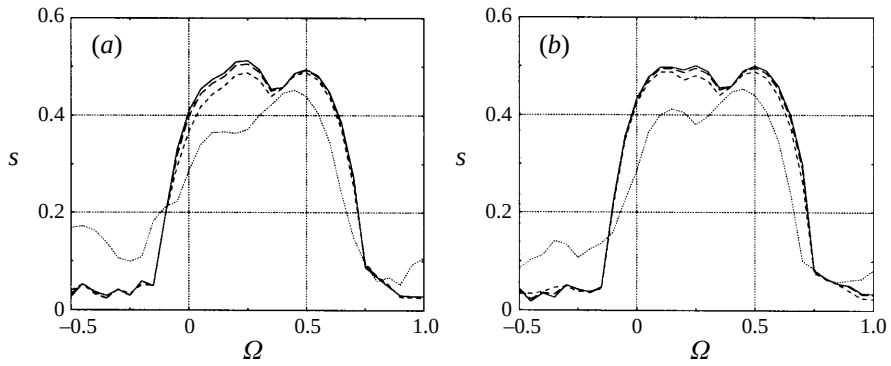

FIGURE 6. Comparison between pressureless (———) and three-dimensional instabilities (⋯⋯ , $k = 10$; ------ , $k = 50$; – – – – , $k = 100$) for $\rho = 1/3$. (*a*) Fundamental modes; (*b*) subharmonic modes.

also obtained by crudely dropping out the pressure term in the complete linear problem (4.3). When the physical problem or the basic flow exhibits a characteristic length scale (the spatial period of the Stuart vortices in the present case), (8.2) is recovered from (8.1) at large wavenumber ($k \to \infty$), leading to short-wave eigenmodes strongly localized on streamlines, as pointed out by Pierrehumbert (1986). Following Bayly (1988), LC97 showed that the behaviour of centrifugal and rotation-induced short-wave instabilities is given at first order by the oversimplified pressureless analysis, and for complex vortical flows, Leblanc (1997) showed its relevance using the geometrical optics stability theory (see further discussions).

In order to avoid confusion, it must be realized that $\boldsymbol{v}(x, y, t)$ in (8.2) is *not* a physical two-dimensional velocity field. Such an interpretation, used by Tritton & Davies (1981) and others with the 'displaced-particle' approach, leads to violation of the incompressibility constraint (see discussion in LC97). The true velocity perturbation is $\boldsymbol{v}'(\boldsymbol{x}, t) = \mathrm{e}^{\mathrm{i}kz}\boldsymbol{v}(x, y, t)$, which is two-component but highly three-dimensional, since the short-wave condition says that the variability with respect to the spanwise coordinate (z) is much higher than the variability with respect to planar coordinates (x, y).

System (8.2) is a linear problem with spatially periodic coefficients and also admits the Floquet representation (5.2). With homogeneous boundary conditions, the pressureless eigenvalue problem

$$(\sigma + \boldsymbol{U}\cdot\nabla)\tilde{\boldsymbol{v}}(x, y) + \boldsymbol{M}\,\tilde{\boldsymbol{v}}(x, y) = 0 \tag{8.3}$$

may be computed numerically and compared to the 'exact' linear problem (5.3) for large wavenumbers. Fundamental and subharmonic eigenmodes of (8.3) admit the same growth rate $s = \mathrm{Re}(\sigma)$ but a different frequency $\omega = \mathrm{Im}(\sigma)$, because the Floquet parameter μ appears only in the convective operator $\boldsymbol{U}\cdot\nabla = \Psi_y(\mathrm{i}\mu + \partial_x) - \Psi_x\partial_y$.

A comparison between three-dimensional short-wave instabilities and pressureless solutions is plotted on figure 6. It is clearly seen that at large wavenumber, fundamental and subharmonic Floquet modes exhibit a comparable temporal behaviour, even in the non-rotating case contrary to the results of Pierrehumbert & Widnall (1982). The slight differences between figures 6(*a*) and 6(*b*) come from the different truncation schemes used for fundamental and subharmonic modes. Possible explanations of the subharmonic cut-off found by Pierrehumbert & Widnall (1982) could be their low resolution, or the domain truncation. Experimental observations of the subharmonic cut-off for secondary instability of Tollmien–Schlichting waves (Herbert

1988) could be a consequence of viscosity (Lagnado *et al.* 1984; Craik & Criminale 1986; Landman & Saffman 1987; Lifschitz 1991; SP94). Figure 6 also shows that the temporal behaviour of short-wave three-dimensional instabilities asymptotes to the pressureless solution.

8.2. *Hyperbolic and elliptical instabilities*

Unbounded flows with a quadratic streamfunction

$$\Psi(x, y) = -\tfrac{1}{2}((\gamma - \epsilon)x^2 + (\gamma + \epsilon)y^2)$$

have been studied extensively in the context of rapid distortion theory (RDT) of homogeneous turbulence in both rotating and non-rotating frames (Batchelor & Proudman 1954; Cambon 1982; Cambon *et al.* 1985; and others) and more recently in the context of hydrodynamic stability theory (Lagnado *et al.* 1984; Craik & Criminale 1986; Pierrehumbert 1986; Bayly 1986; Landman & Saffman 1987; Craik 1989; Waleffe 1989, 1990; and others). The close links between these two approaches are reviewed by Cambon *et al.* (1994). In particular, both allow a wave-like perturbation with a time-dependent wave vector to be sought:

$$[\boldsymbol{u}', \pi'](\boldsymbol{x}, t) = \mathrm{e}^{\mathrm{i}\boldsymbol{k}(t)\cdot\boldsymbol{x}}[\boldsymbol{u}, \pi](t),$$

where the projection on the (x, y)-plane of $\boldsymbol{k}(t)$ is denoted by $\boldsymbol{\alpha}(t)$, which is a solution of

$$\dot{\boldsymbol{\alpha}} = -\boldsymbol{N}^T\boldsymbol{\alpha}$$

with $\boldsymbol{N} = \nabla\boldsymbol{U}$ given by (3.2), whereas its spanwise component $k = \boldsymbol{k}(t)\cdot\boldsymbol{e}_z$ is constant. The physical interpretation is that the wave vector follows the deformation induced by the basic flow, so that its initial value $\boldsymbol{k}(0) = \boldsymbol{K}$ is related to Lagrangian coordinates (Cambon *et al.* 1985, 1994).

The 'motion' of $\boldsymbol{\alpha}(t)$ is easily integrated for the three classes of flows (elliptical, hyperbolic or pureshear). Substitution into the Euler equation (linearized or not since each single mode verifies $\boldsymbol{u}' \cdot \nabla\boldsymbol{u}' = 0$) leads to a linear system with time-dependent coefficients that may be written in the following form:

$$\dot{\boldsymbol{v}} + \boldsymbol{M}\boldsymbol{v} = \boldsymbol{\alpha}\boldsymbol{\alpha}^T/|\boldsymbol{k}|^2(\boldsymbol{M} + \boldsymbol{N})\boldsymbol{v}. \tag{8.4}$$

$\boldsymbol{M}$ is the inertial tensor defined by (4.4), $\boldsymbol{v}(t)$ is the projection of $\boldsymbol{u}(t)$ on the (x, y)-plane, and the time-dependent right-hand side of (8.4) is the contribution of the pressure perturbation. Equation (8.4) may be analytically integrated for some particular initial conditions on $\boldsymbol{\alpha}(t)$ (see Cambon 1982; Cambon *et al.* 1985, 1994 for RDT, and Lagnado *et al.* 1984; Craik & Criminale 1986 for hydrodynamic stability). In the elliptical case, it seems to the authors that the first evidence of an instability appears in Cambon's (1982) thesis (see also figures 4–6 in Cambon *et al.* 1985), even though Bayly (1986) was the first to perform a Floquet analysis, taking advantage of time-periodicity of the coefficients involved in the right-hand side of (8.4). His results confirmed the spectral calculations of Pierrehumbert (1986) who concluded that the so-called 'elliptical instability' was a generic mechanism for secondary instability in shear flows, as soon as the streamlines of the non-parallel basic flow exhibit elliptical regions (see the review by Bayly *et al.* 1988). This has been commonly accepted and the structure of the localized eigenmodes of the elliptical instability (Pierrehumbert 1986; Waleffe 1989, 1990) was in good agreement with three-dimensional secondary instabilities of shear flows with non-parallel streamlines (Orszag & Patera 1981, 1983; Pierrehumbert & Widnall 1982; Klaassen & Peltier 1985, 1989, 1991; Lundgren &

Mansour 1996; Sipp & Jacquin 1997). This is the 'core' mode of SP94. The recent experiments of Leweke & Williamson (1998) show nicely the birth of the elliptical instability in the cores of a dipole.

During the past decade, from a theoretical point of view, the role of hyperbolic regions for secondary instability has been completely omitted, contrary to RDT which predicts that hyperbolic regions for the 'mean field' are well-known to be places where intense 'production' of turbulent kinetic energy occurs (Batchelor & Proudman 1954; Cambon 1982; Cambon *et al.* 1985, 1994). However, recently Friedlander & Vishik (1991) showed with the 'geometrical optics' stability methods (see also Lifschitz & Hameiri 1991) that in an inertial frame any inviscid incompressible flow with a hyperbolic stagnation point is unstable, confirming the results of Lagnado *et al.* (1984) for unbounded quadratic flows with hyperbolic streamlines. The 'hyperbolic instability' corresponds of course to the 'braid' mode identified by SP94 (see their figure 14) which was shown to be dominant in the non-rotating case. According to Klaassen & Peltier (1985, 1989, 1991), hyperbolic (or braid) instability is closely linked to the longitudinal vortices (or 'ribs') in secondary instabilities of mixing layers (see for example Ho & Huerre 1984; Metcalfe *et al.* 1987; Lasheras & Choi 1988). The mechanism of vortex line stretching in the plane of the basic flow, *"along the principal axis of extensional strain"* well depicted by Lagnado *et al.* (1984), and also known in RDT works, appears to be a generic mechanism in inviscid and viscous flows: in the wake of a cylinder, Williamson (1996) observed experimentally his 'mode B', and by direct numerical simulations, Leblanc & Godeferd (1997) pointed out that two-dimensional Taylor–Green cells with a square aspect ratio (no elliptical cores) perturbed three-dimensionally lead to the formation of 'vortex fingers' in the hyperbolic regions. This is confirmed by stability analyses (Sipp & Jacquin 1997).

As first pointed out by Cambon (1982) in the RDT context, very simple solutions of (8.4) may be found when the time-dependent right-hand side vanishes. Such modes correspond to a constant pure spanwise wave vector $\boldsymbol{k}(t) = (0, 0, k)$ which is satisfied for the initial condition $\boldsymbol{\alpha}(0) = 0$. The pressure field plays no role in these instabilities, which are solutions of

$$\dot{\boldsymbol{v}} + \boldsymbol{M}\,\boldsymbol{v} = 0$$

and which take the simple form $\boldsymbol{v}'(\boldsymbol{x}, t) = \mathrm{e}^{\sigma t}\mathrm{e}^{\mathrm{i}kz}\boldsymbol{v}_0$ with

$$\sigma = (\epsilon^2 - \gamma_t^2)^{1/2} \tag{8.5}$$

where $\gamma_t = \gamma + 2\Omega$ is half the tilting vorticity of the quadratic flow. These pressureless (but nevertheless exact) perturbations are amplified if $|\epsilon| > |\gamma + 2\Omega|$ and neutral otherwise. Because of the fact that they are not spatially localized in the (x, y)-plane these pressureless disturbances seem to have no physical interpretation. Obviously, without the Coriolis force, they are neutral in the elliptical case $|\gamma| > |\epsilon|$: instability occurs for oblique wave vectors (Bayly 1986). But, according to Lagnado *et al.* (1984) they are amplified in the hyperbolic case $|\gamma| < |\epsilon|$. Furthermore, in a rotating frame, they are amplified when the rotation rate lies in the range

$$|\gamma| - |\epsilon| < 2\Omega < |\gamma| + |\epsilon|,$$

where, without lost of generality, ϵ and γ are negative in order to be consistent with (3.3). And, over this bandwidth, numerical integration of the Floquet problem (8.4) for the elliptical case by Cambon *et al.* (1994) showed that they are the most amplified (see their figure 4*c–e*). By inspection of the equation for the vorticity perturbation, they showed that the zero absolute vorticity case ($\gamma + \Omega = 0$) is neutral if $|\gamma| \geqslant |\epsilon|$.

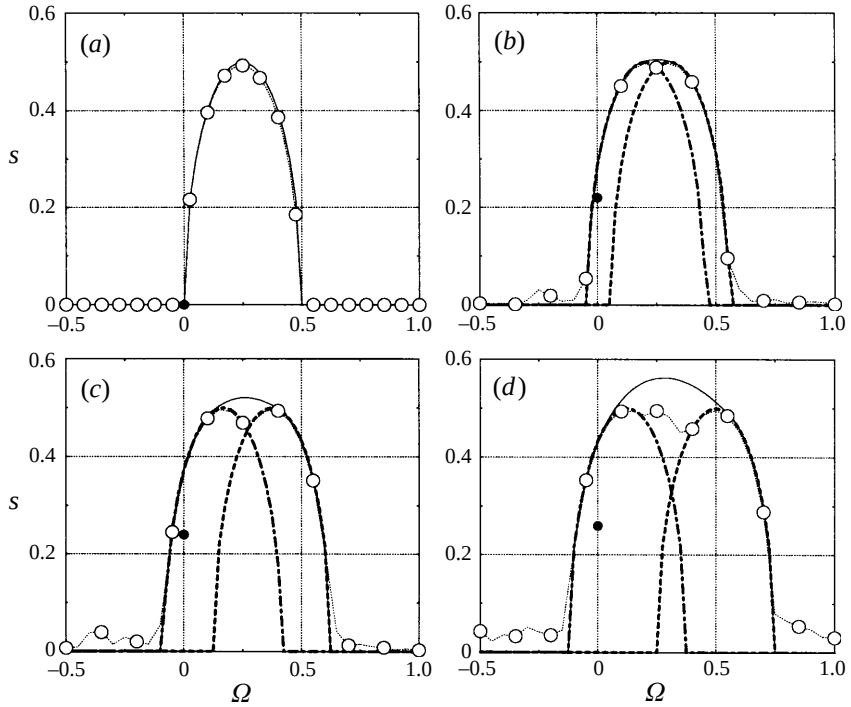

FIGURE 7. Comparison between subharmonic instabilities for $k = 100$ (·····○·····), quadratic instabilities with pure spanwise wavevector (–·–·–, hyperbolic; ------, elliptical) and the instability criterion (———). (*a*) $\rho = 0$; (*b*) $\rho = 1/10$; (*c*) $\rho = 1/5$; (*d*) $\rho = 1/3$. The • correspond to the maximum growth rate of elliptical instability with time-dependent wavevector (from Landman & Saffman 1987).

8.3. *Mode selection by rotation: the tuning effect*

The role of these quadratic instabilities for the Stuart vortices is illustrated on figure 7. The analytical growth rate of perturbations with pure spanwise wave vector (8.5) is plotted for hyperbolic regions and elliptical cores characterized by (3.2) and (3.3). Comparison is made with short-wave three-dimensional subharmonic eigenmodes of the Stuart vortices. The two maxima of instability in the unstable range, also observed on figures 4 and 6 at large spanwise wavenumber k, correspond in fact to two distinct mechanisms which compete: namely hyperbolic and elliptical instabilities. For weak cyclonic and anticyclonic rotations, short-wave instabilities reside in the hyperbolic region, as in the non-rotating case. This instability is replaced by the elliptical one for stronger anticyclonic rotation ($\Omega > 0$). This illustrates again the 'tuning' effect of the Coriolis force, which selects and/or kills instability.

In the non-rotating case, the maximum growth rate of elliptical instability with an oblique time-dependent wave vector is also plotted on figure 7. The results are from figure 1 in Landman & Saffman (1987): their eccentricity parameter 'β' corresponds to ϵ/γ given by (3.3) for elliptical cores, and their dimensionless growth rate 'σ_I' has to be multiplied by γ. Recall that Waleffe (1989, 1990) has shown that, at small eccentricity, the dimensionless growth rate behaves as $\frac{9}{16}\epsilon/\gamma$. For the Stuart vortices, figure 7 is an illustration that for short waves, instability is governed by hyperbolic regions rather than elliptical cores, as previously shown qualitatively by SP94. This result does not call the 'universality' of elliptical instability in question, but it simply

shows the crucial role of hyperbolic stagnation points completely omitted in the basic mechanisms of secondary instabilities in shear flows (see for example Bayly *et al.* 1988).

When $\rho = 0$ (figure 7*a*), the calculations correspond to oblique waves with $\alpha = 1/2$ of the hyperbolic-tangent mixing layer, studied first by Johnson (1963) and then reconsidered by Yanase *et al.* (1993) including viscous effects. The parallel basic flow no longer exhibits elliptical or hyperbolic stagnation points, and the two distinct instability bandwidths are lost in the range $0 < \Omega < 1/2$, consistent with the Pedley criterion. The behaviour of short-wave oblique modes is similar to instabilities with a pure spanwise wave vector (figure 1), and this short-wavelength behaviour is given by the pressureless analysis (LC97). In the viscous case, a cut-off should happen above a critical spanwise wavenumber, as pointed out for quadratic flows by Lagnado *et al.* (1984), Craik & Criminale (1986) and Landman & Saffman (1987). For non-homogeneous flows this viscous cut-off mechanism leads to a preferred spanwise wavenumber at which instability occurs (Yanase *et al.* 1993; SP94). The same mechanism also occurs in classical Rayleigh–Taylor instability (see Drazin & Reid 1981) for which viscosity selects the critical spanwise wavenumber.

8.4. *The Lifschitz & Hameiri theory*

The geometrical optics stability theory for short-wave instabilities developed by Lifschitz & Hameiri (1991) may be applied to rotating fluids (Bayly *et al.* 1996; Lebovitz & Lifschitz 1996; Leblanc 1997). This powerful alternative to classical stability methods consists in seeking the perturbation in the WKB form:

$$[\boldsymbol{u}', \pi'](\boldsymbol{x}, t) = \mathrm{e}^{\mathrm{i}\phi(\boldsymbol{x},t)/\epsilon}[\boldsymbol{a}, \pi](\boldsymbol{x}, t) + O(\epsilon)$$

where ϵ is a small parameter, $\phi(\boldsymbol{x}, t)$ is the phase field (real-valued) and $\boldsymbol{a}(\boldsymbol{x}, t)$ is the complex amplitude. The above expansion also contains terms of order ϵ (Lifschitz & Hameiri 1991), not written here for brevity. Injecting into the linearized equations (4.2) or (4.3) and equating the different order terms yields (after elimination of pressure by applying the 'projector' familiar to the turbulence community)

$$\mathrm{D}_t \phi = 0:$$

the phase field is convected by the basic flow. Introducing the wave vector $\boldsymbol{k}(\boldsymbol{x}, t) = \nabla\phi$, $\boldsymbol{\alpha}(\boldsymbol{x}, t)$, its projection on the (x, y)-plane, and $\boldsymbol{v}(\boldsymbol{x}, t)$, the projection of $\boldsymbol{a}(\boldsymbol{x}, t)$, the linear problem (4.3) now reads

$$\mathrm{D}_t \boldsymbol{\alpha} = -\boldsymbol{N}^T \boldsymbol{\alpha},$$
$$\mathrm{D}_t \boldsymbol{v} + \boldsymbol{M}\boldsymbol{v} = \boldsymbol{\alpha}\boldsymbol{\alpha}^T/|\boldsymbol{k}|^2(\boldsymbol{M} + \boldsymbol{N})\boldsymbol{v},$$

which is a set of partial differential equations evolving along the trajectories of the basic flow. This system is analogous to 'Kelvin's' set of equations for quadratic flows (8.4), except that the coefficients are no longer constant but are space-dependent. Introducing a Lagrangian representation, the above system is reduced to a system of ordinary differential equations that may be solved sequentially for suitable initial data. The remarkable idea of the geometrical optics stability theory lies in the fact that the instability is localized along a trajectory of the basic flow (such as stagnation points for example), and vanishes outside, so that the stability problem frees itself of the boundary conditions. This concept was also introduced in Bayly (1988, 1989). Lifschitz & Hameiri (1991) showed that *a sufficient condition for instability is that* $|\boldsymbol{a}(\boldsymbol{X}, t)| \to \infty$ *when* $t \to \infty$ *along the trajectory* $\boldsymbol{X}$.

They showed that *any steady flow in an inertial frame is unstable if it contains a stagnation point (hyperbolic, elliptical or pure shear)*. In a rotating flow, the conclusion is not straightforward, since the Coriolis force may have killed three-dimensional instabilities (at zero absolute vorticity for a vortex core for example). Leblanc (1997) showed that for pure spanwise wave vectors $\boldsymbol{k}(\boldsymbol{x}, t) = k\boldsymbol{e}_z$, the pressureless problem (8.2) makes sense, and that *the flow is unstable if* $\Phi(x_0, y_0) < 0$ *on a stagnation point located at* (x_0, y_0) (Φ is the general discriminant). This sufficient stability condition was used to show that Chaplygin's dipole (see Meleshko & van Heijst 1994) moving along a circular path is unstable.

Concerning Stuart vortices, on the stagnation points, the general discriminant (4.5) reads

$$\Phi_E = (2\Omega - \rho/(1-\rho))(2\Omega - 1/(1-\rho)),$$
$$\Phi_H = (2\Omega + \rho/(1+\rho))(2\Omega - 1/(1+\rho)),$$

and the growth rate (in both Lagrangian and Eulerian representations) of these short-wave instabilities is $(-\Phi_{E,H})^{1/2}$, identical to the growth rate of the quadratic modes given by (8.5), and plotted on figure 7. This provides a direct link between this recent theory and the classical spectral methods.

8.5. *Towards a general criterion for complex flows?*

Finally, LC97 suggested that the extended criterion could be valuable for any complex vortical flow, that is to say $\Phi(x, y) < 0$ somewhere implies instability. The starting point is the pressureless equation (8.2), which, in a Lagrangian representation, involves time-dependent coefficients. If the streamlines are closed, a Floquet analysis on streamlines is needed (Bayly 1988, 1989; Sipp & Jacquin 1997).

The pressureless problem (8.2) involves the convective operator $\boldsymbol{U} \cdot \nabla(\ )$. Obviously, if it cannot be dropped out or diagonalized on the same basis as the inertial tensor, as pointed out by Bayly (1988), nothing can be concluded on the temporal behaviour of the perturbations, even for pressureless modes. On figure 7 (thin solid lines) is plotted the maximum temporal growth rate of the simple linear problem $\partial_t \boldsymbol{v} + \boldsymbol{M}\,\boldsymbol{v} = 0$, given by

$$\max_{(x,y)} [-\Phi(x, y)]^{1/2}.$$

It is seen that the criterion is in good agreement with the linear stability calculations: the unstable bandwidth includes the two kinds of instability (hyperbolic and elliptical). The magnitude of the growth rate of short-wave (or pressureless) modes is also in good agreement with the theoretical predictions. This is perhaps an anecdotal result, but this criterion has been also tested successfully on Taylor–Green cells and Mallier–Maslowe vortices, both in rotating and inertial frames.

This illustrates the role of the convective operator in linear stability of complex vortical flows. Recall that for simple rotating flows (parallel shear flows, circular vortices and quadratic flows), the convective operator may always be dropped out by a convenient choice of the wave vector of the perturbation, and thus the growth of short-wave or pressureless unstable modes is governed exactly by the above expression.

9. Rapid rotation

9.1. *Stabilization*

Under rapid rotation (cyclonic or anticyclonic), the unstable band is narrowed down to the $k = 0$ axis, as illustrated by figure 8(*a*). Three-dimensional instabilities are

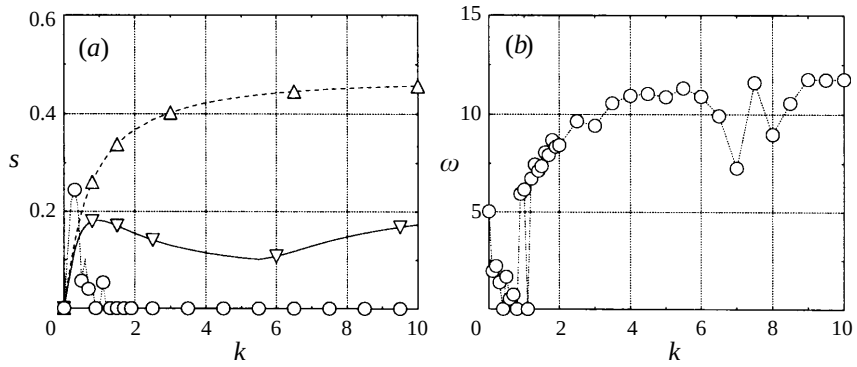

FIGURE 8. Fundamental modes for $\rho = 1/10$ under various rotations (—▽—, $\Omega = 0$; ---△---, $\Omega = 1/4$; ····○····, $\Omega = 5$). (*a*) Growth rate; (*b*) frequency.

thus stabilized by strong rotation rates, and only two-dimensional Floquet modes (unaffected by the Coriolis force) survive (the subharmonic ones). This may be interpreted as a manifestation of the Taylor–Proudman theorem, as discussed recently by SP94 and Carnevale *et al.* (1997). For an elliptical vortex core, Lebovitz & Lifschitz (1996) have shown that instability is killed in the limit $\Omega \to \infty$.

Following Batchelor (1967, p. 558), the Taylor–Proudman theorem states that: *steady motions at small Rossby number* (*rapid rotation*) *must be a superposition of a two-dimensional motion in the* (x, y)*-plane and a spanwise motion which is independent of* z. As mentioned in the Introduction, transition to two-dimensional turbulence and the emergence of vortices is outside its scope, because it involves complex nonlinear mechanisms. Indeed, for homogeneous rotating turbulence, the two-dimensionalization is equivalent to a concentration of the spectral density of energy towards the 'two-dimensional manifold' characterized by $\boldsymbol{k} \cdot \boldsymbol{\Omega} = 0$, where $\boldsymbol{k}$ is the three-dimensional wave vector in spectral space. From a spectral standpoint, the Taylor–Proudman theorem only says that the 'slow manifold' (the stationary mode of the linear regime) is the two-dimensional one ($\boldsymbol{k} \cdot \boldsymbol{\Omega} = 0$), but explaining the nonlinear angular drain of energy towards the two-dimensional manifold is outside its scope (see Waleffe 1993; Babin *et al.* 1996; Cambon *et al.* 1997).

Figure 8(*a*) also illustrates the destabilizing influence of the Coriolis force for a weak anticyclonic rotation, compared to the non-rotating case. This latter case ($\Omega = 0$) illustrates again the role of the instability linked to the hyperbolic stagnation points which becomes dominant for short-wave instability ($k > 5.5$, above which s increases with k), whereas the destabilizing case ($\Omega = 1/4$) is still dominated by the elliptical modes.

9.2. *Inertial waves*

Even though three-dimensional modes tend to be neutral ($s = \mathrm{Re}(\sigma) \to 0$) under rapid rotation, their frequency $\omega = \mathrm{Im}(\sigma)$ is close to 2Ω, as illustrated by figure 8(*b*). This is not really surprising since for short-wave instabilities $k \gg 1$ at large rotation rate $|\Omega| \gg k$, crudely neglecting all gradient terms, the spectral problem reduces to

$$\sigma \tilde{\boldsymbol{v}}(x, y) + \boldsymbol{C}\, \tilde{\boldsymbol{v}}(x, y) = 0$$

with $\boldsymbol{C}$ the Coriolis tensor defined in (4.4). The eigenvalues are $\sigma = \pm 2\Omega \mathrm{i}$. These neutral modes may be interpreted as inertial waves (Greenspan 1969). Indeed, in an unbounded flow at rest in a rotating frame, plane inertial waves propagate, with

dispersion law $\omega = \pm 2\Omega \cos\theta$, where θ is the angle between the (constant) wave vector and the rotation axis.

For a wave vector aligned with the rotation axis, the frequency is $\omega = \pm 2\Omega$; the pressure field plays no role and the group velocity vanishes, showing that such inertial waves, do not propagate energy. Figure 8 seems to establish their existence. Recently, Carnevale *et al.* (1997) observed similar inertial waves for circular vortices subjected to rapid rotation.

10. Conclusion

A detailed investigation of the effects of the Coriolis force on the three-dimensional linear instabilities of Stuart vortices has been performed. This exact inviscid solution describes an array of co-rotating vortices embedded in a shear flow. When the axis of rotation is perpendicular to the plane of the basic flow, the stability analysis consists of an eigenvalue problem for non-parallel versions of the coupled Orr–Sommerfeld and Squire equations, which has been solved numerically by a spectral method.

The results may be summarized as follows:

Stabilization and destabilization: as observed in various experiments and as shown analytically for simple basic flows (circular vortices, parallel shear flows, unbounded quadratic flows), the Coriolis force plays a stabilizing or a destabilizing role, compared to the non-rotating case. Strong anticyclones are unstable.

Short-wave breakdown: in the unstable range, three-dimensional inviscid instabilities are promoted, and at large spanwise wavenumber, their temporal growth rate asymptotes to a constant value, given by the pressureless analysis. This short-wave (in the spanwise direction) behaviour is consistent with analytical results for centrifugal and rotation-induced instabilities.

Hyperbolic and elliptical instabilities: they are generated by the stagnation points of Stuart's streamfunction and compete under the effect of the Coriolis force. In particular, for the non-rotating case, both fundamental and subharmonic Floquet modes exhibit a growth rate given by the stability of the unbounded quadratic flow with hyperbolic streamlines. On the other hand, for weak anticyclonic rotation, the short-wave eigenmodes behave like the instability of the unbounded elliptical vortex subjected to rotation.

The Lifschitz & Hameiri theory: the geometrical optics stability method gives a theoretical background to the results described above, since it considers the local topological properties of the basic flow. When applied to stagnation points, the stability properties of quadratic flows are recovered. This provides finally a link between various fields of investigation in fluid mechanics, i.e. hydrodynamic stability theory (via spectral methods) and turbulence modelling (via RDT).

General discriminant: the second invariant of the inertial tensor (the sum of the basic velocity gradient and of the Coriolis tensor) gives a good prediction of the bandwidth of unstable short-wave perturbations (with or without the Coriolis force). Recall that it gives the exact bounds on stagnation points and for simple basic flows (circular vortices, parallel shear flows, unbounded quadratic flows).

Inertial waves: under a rapid cyclonic or anticyclonic rotation (weak Rossby number), three-dimensional instabilities become neutral, and owing to their frequency, they can be interpreted as inertial waves. A similar behaviour has been found for monopolar vortices subjected to strong rotation. Two-dimensional instabilities (pairing modes) are of course unaffected by the Coriolis force.

All these features could be generic to the linear stability of two-dimensional

inviscid vortices in a rotating fluid. The Coriolis force appears to be a catalyst of short-wavelength and/or pressureless modes, which are tuned (resp. detuned) for a destabilizing (resp. stabilizing) rotation.

We are grateful to Dr Alex Joia for reading this manuscript, and to Professor Julian Scott for advice and help. Dr Denis Sipp is also warmly acknowledged for fruitful discussions. S. L. was supported by the M. E. N. E. S. R.

REFERENCES

Babin, A., Mahalov, A. & Nicolaenko, B. 1996 Global splitting, integrability and regularity of 3D Euler and Navier–Stokes equations for uniformly rotating fluids. *Eur. J. Mech.* B/*Fluids* **15**, 291–300.

Batchelor, G. K. 1967 *An Introduction to Fluid Dynamics*. Cambridge University Press.

Batchelor, G. K. & Proudman, I. 1954 The effect of rapid distortion on a fluid in turbulent motion. *Q. J. Mech. Appl. Maths* **7**, 83–103.

Bayly, B. J. 1986 Three-dimensional instability of elliptical flow. *Phys. Rev. Lett.* **57**, 2160–2163.

Bayly, B. J. 1988 Three-dimensional centrifugal-type instabilities in inviscid two-dimensional flows. *Phys. Fluids* **31**, 56–64.

Bayly, B. J. 1989 Computations of broad band instabilities in a class of quasi-two-dimensional flows. In *Mathematical Aspects of Vortex Dynamics* (ed. R. E. Caflisch), pp. 50–58. Philadelphia: SIAM.

Bayly, B. J., Holm, D. D. & Lifschitz, A. 1996 Three-dimensional stability of elliptical vortex columns in external strain flows. *Phil. Trans. R. Soc. Lond.* A **354**, 895–926.

Bayly, B. J., Orszag, S. A. & Herbert, T. 1988 Instability mechanisms in shear-flow transition. *Ann. Rev. Fluid Mech.* **20**, 359–391.

Bidokhti, A. A. & Tritton, D. J. 1992 The structure of a turbulent free shear layer in a rotating fluid. *J. Fluid Mech.* **241**, 469–502.

Bottaro, A., Klingmann, G. B. & Zebib, A. 1996 Görtler vortices with system rotation. *Theor. Comput. Fluid Dyn.* **8**, 325–347.

Cambon, C. 1982 Etude spectrale d'un champ turbulent incompressible soumis à des effets couplés de déformation et de rotation imposés extérieurement. PhD thesis, Université de Lyon I, France.

Cambon, C., Benoît, J.-P., Shao, L. & Jacquin, L. 1994 Stability analysis and large eddy simulation of rotating turbulence with organized eddies. *J. Fluid Mech.* **278**, 175–200.

Cambon, C., Mansour, N. N. & Godeferd, F. S. 1997 Energy transfer in rotating turbulence. *J. Fluid Mech.* **337**, 303–332.

Cambon, C., Teissèdre, C. & Jeandel, D. 1985 Etude d'effets couplés de déformation et de rotation sur une turbulence homogène. *J. Méc. Théor. Appl.* **4** 629–657.

Canuto, C., Hussaini, M. Y., Quarteroni, A. & Zang, T. A. 1988 *Spectral Methods in Fluid Dynamics*. Springer.

Carnevale, G. F., Briscolini, M., Kloosterziel, R. C. & Vallis, G. K. 1997 Three-dimensionally perturbed vortex tubes in a rotating flow. *J. Fluid Mech.* **341**, 127–163.

Carnevale, G. F. & Kloosterziel, R. C. 1994 Emergence and evolution of triangular vortices. *J. Fluid Mech.* **259**, 305–331.

Craik, A. D. D. 1989 The stability of unbounded two- and three-dimensional flows subject to body forces: some exact solutions. *J. Fluid Mech.* **198**, 275–292.

Craik, A. D. D. & Criminale, W. O. 1986 Evolution of wavelike disturbances in shear flows: a class of exact solutions of the Navier–Stokes equations. *Proc. R. Soc. Lond.* A **406**, 13–26.

Dowling, T. E. 1995 Dynamics of jovian atmospheres. *Ann. Rev. Fluid Mech.* **27**, 293–334.

Drazin, P. G. & Reid, W. H. 1981 *Hydrodynamic Stability*. Cambridge University Press.

Friedlander, S. & Vishik, M. M. 1991 Instability criteria for the flow of an inviscid incompressible fluid. *Phys. Rev. Lett.* **66**, 2204–2206.

Gledzer, E. B. & Ponomarev, V. M. 1992 Instability of bounded flows with elliptical streamlines. *J. Fluid Mech.* **240**, 1–30.

Greenspan, H. P. 1969 *The Theory of Rotating Fluids*. Cambridge University Press.

Heijst, G. J. F. van, Kloosterziel, R. C. & Williams, C. W. M. 1991 Laboratory experiments on the tripolar vortex in a rotating fluid. *J. Fluid Mech.* **225**, 301–322.

Henningson, D. 1995 Bypass transition and linear growth mechanisms. In *Advances in Turbulence V* (ed. R. Benzi), pp. 190–204. Kluwer.

Herbert, T. 1983 Secondary instability of plane channel flow to subharmonic three-dimensional disturbances. *Phys. Fluids* **26**, 871–874.

Herbert, T. 1988 Secondary instability of boundary layers. *Ann. Rev. Fluid Mech.* **20**, 487–526.

Herbert, T., Bertolotti, F. P. & Santos, G. R. 1987 Floquet analysis of secondary instability in shear flows. In *Proc. ICASE/NASA Workshop Stability Time-Dependent Spatially Varying Flows* (ed. D. L. Dwoyer & M. Y. Hussaini), pp. 43–57. Springer.

Ho, C.-M. & Huerre, P. 1984 Perturbed free shear layers. *Ann. Rev. Fluid Mech.* **16**, 365–424.

Hopfinger, E. J., Browand, F. K. & Gagne, Y. 1982 Turbulence and waves in a rotating tank. *J. Fluid Mech.* **125**, 505–534.

Hopfinger, E. J. & Heijst, G. J. F. van 1993 Vortices in rotating fluids. *Ann. Rev. Fluid Mech.* **25**, 241–289.

Johnson, J. A. 1963 The stability of shearing motion in a rotating fluid. *J. Fluid Mech.* **17**, 337–352.

Kelly, R. E. 1967 On the stability of an inviscid shear layer which is periodic in space and time. *J. Fluid Mech.* **27**, 657–689.

Klaassen, G. P. & Peltier, W. R. 1985 The onset of turbulence in finite-amplitude Kelvin–Helmholtz billows. *J. Fluid Mech.* **155**, 1–35.

Klaassen, G. P. & Peltier, W. R. 1989 The role of transverse secondary instabilities in the evolution of free shear layers. *J. Fluid Mech.* **202**, 367–402.

Klaassen, G. P. & Peltier, W. R. 1991 The influence of stratification on secondary instability in free shear layers. *J. Fluid Mech.* **227**, 71–106.

Kloosterziel, R. C. 1990 Barotropic vortices in a rotating fluid. PhD thesis, University of Utrecht, The Netherlands.

Kloosterziel, R. C. & Heijst, G. J. F. van 1991 An experimental study of unstable barotropic vortices in a rotating fluid. *J. Fluid Mech.* **223**, 1–24.

Lagnado, R. R., Phan-Thien, N. & Leal, L. G. 1984 The stability of two-dimensional linear flows. *Phys. Fluids* **27**, 1094–1101.

Lamb, H. 1932 *Hydrodynamics*. Cambridge University Press.

Landman, M. J. & Saffman, P. G. 1987 The three-dimensional instability of strained vortices in a viscous fluid. *Phys. Fluids* **30**, 2339–2342.

Lasheras, J. C. & Choi, H. 1988 Three-dimensional instability of a plane free shear layer: an experimental study of the formation and evolution of streamwise vortices. *J. Fluid Mech.* **189**, 53–86.

Leblanc, S. 1997 Stability of stagnation points in rotating flows. *Phys. Fluids* **9**, 3566–3569.

Leblanc, S. & Cambon, C. 1996 Stability of the Stuart vortices in a rotating frame. In *Advances in Turbulence VI* (ed. S. Gavrilakis, L. Machiels & P. A. Monkewitz), pp. 351–354. Dordrecht: Kluwer.

Leblanc, S. & Cambon, C. 1997 On the three-dimensional instabilities of plane flows subjected to Coriolis force. *Phys. Fluids* **9**, 1307–1316 (referred to herein as LC97).

Leblanc, S. & Godeferd, F. S. 1997 Coherence of vortices in a rotating fluid. In *Proc. Eleventh Symp. on Turbulent Shear Flows, Grenoble, France*.

Lebovitz, N. R. & Lifschitz, A. 1996 Short-wavelength instabilities of Riemann ellipsoids. *Phil. Trans. R. Soc. Lond.* A **354**, 927–950.

Lesieur, M., Yanase, S. & Métais, O. 1991 Stabilizing and destabilizing effects of a solid-body rotation on quasi-two-dimensional shear layers. *Phys. Fluids* A **3**, 403–407.

Leweke, T. & Williamson, C. H. K. 1998 Coupled elliptic instability of a vortex pair. *J. Fluid Mech.* (in press).

Lifschitz, A. 1991 Short wavelength instabilities of incompressible three-dimensional flows and generation of vorticity. *Phys. Lett.* A **157**, 481–487.

Lifschitz, A. 1994 On the stability of certain motions of an ideal incompressible fluid. *Adv. Appl. Maths* **15**, 404–436.

Lifschitz, A. & Hameiri, E. 1991 Local stability conditions in fluid dynamics. *Phys. Fluids* A **3** 2644–2651.

Lollini, L. 1997 Ondes et turbulence dans un écoulement confiné en rotation. PhD thesis, Ecole Centrale de Lyon, France.

Lundgren, T. S. & Mansour, N. N. 1996 Transition to turbulence in an elliptic vortex. *J. Fluid Mech.* **307**, 43–62.

Marcus, P. S. 1993 Jupiter's Great Red Spot and other vortices. *Ann. Rev. Astron. Astrophys.* **31**, 523–573.

Meleshko, V. V. & Heijst, G. J. F. van 1994 On Chaplygin's investigations of two-dimensional vortex structures in an inviscid fluid. *J. Fluid Mech.* **272**, 157–182.

Metcalfe, R. W., Orszag, S. A., Brachet, M. E., Menon, S. & Riley, J. J. 1987 Secondary instability of a temporally growing mixing layer. *J. Fluid Mech.* **184**, 207–243.

Michalke, A. 1964 On the inviscid instability of the hyperbolic-tangent velocity profile. *J. Fluid Mech.* **19**, 543–556.

Mutabazi, I., Normand, C. & Wesfreid, J. E. 1992 Gap size effects on centrifugally and rotationally driven instabilities. *Phys. Fluids* A **4**, 1199–1205.

Orszag, S. A. & Patera, A. T. 1981 Subcritical transition to turbulence in planar shear flows. In *Transition and Turbulence* (ed. R. E. Meyer), pp. 127–146. Academic.

Orszag, S. A. & Patera, A. T. 1983 Secondary instability of wall-bounded shear flows. *J. Fluid Mech.* **128**, 347–385.

Pedley, T. J. 1969 On the stability of viscous flow in a rapidly rotating pipe. *J. Fluid Mech.* **35**, 97–115.

Pierrehumbert, R. T. 1986 Universal short-wave instability of two-dimensional eddies in an inviscid fluid. *Phys. Rev. Lett.* **57**, 2157–2159.

Pierrehumbert, R. T. & Widnall, S. E. 1982 The two- and three-dimensional instabilities of a spatially periodic shear layer. *J. Fluid Mech.* **114**, 59–82.

Sipp, D. & Jacquin, L. 1997 Elliptic instability in 2D-flattened Taylor–Green vortices. Submitted to *Phys. Fluids*.

Smyth, W. D. & Peltier, W. R. 1994 Three-dimensionalization of barotropic vortices on the f-plane. *J. Fluid Mech.* **265**, 25–64 (referred to herein as SP94).

Stuart, J. T. 1967 On finite amplitude oscillations in laminar mixing layers. *J. Fluid Mech.* **29**, 417–440.

Tritton, S. C. & Davies, P. A. 1981 Instabilities in geophysical fluid dynamics. In *Hydrodynamic Instabilities and the Transition to Turbulence* (ed. H. L. Swinney & J. P. Gollub), pp. 229–270. Springer.

Waleffe, F. 1989 The 3D instability of a strained vortex and its relation to turbulence. PhD thesis, Massachusetts Institute of Technology, USA.

Waleffe, F. 1990 On the three-dimensional instability of strained vortices. *Phys. Fluids* A **2**, 76–80.

Waleffe, F. 1993 Inertial transfers in the helical decomposition. *Phys. Fluids* A **5**, 677–685.

Waleffe, F. 1995 Hydrodynamic stability and turbulence: beyond transients to a self-sustaining process. *Stud. Appl. Maths* **95**, 319–343.

Williamson, C. H. K. 1996 Three-dimensional wake transition. *J. Fluid Mech.* **328**, 345–407.

Yanase, S., Flores, C., Métais, O. & Riley, J. J. 1993 Rotating free-shear flows. I. Linear stability analysis. *Phys. Fluids* A **5**, 2725–2737.